Modelling double skin façades (DSFs) in whole-building energy simulation tools: Validation and inter-software comparison of naturally ventilated single-story DSFs

Building and Environment 231 (2023) 110002

Contents lists available at ScienceDirect

Building and Environment

journal homepage: www.elsevier.com/locate/buildenv

Modelling double skin façades (DSFs) in whole-building energy simulation tools: Validation and inter-software comparison of naturally ventilated single-story DSFs

Giovanni Gennaro [a,b], Elena Catto Lucchino [c], Francesco Goia [c], Fabio Favoino [a,*]

[a] Department of Energy, Technology Energy Building Environment Research Group, Politecnico di Torino, Torino, Italy
[b] Institute for Renewable Energy, EURAC Research, Bolzano, Italy
[c] Department of Architecture and Technology, Norwegian University of Science and Technology, NTNU, Trondheim, Norway

ARTICLE INFO

Keywords:
Inter-software comparison
Empirical validation
Double skin façade
Naturally ventilated cavities
EnergyPlus
TRNSYS
IDA-ICE
IES-VE

ABSTRACT

Building energy simulation (BES) tools offer the possibility to integrate double skin façade (DSF) technologies into whole building simulation through dedicated modules or possible workarounds. However, the reliability of such tools in predicting the dynamic heat and mass transfer processes within the DSFs is still to be determined. Therefore, this paper aims to assess the performance of four popular BES tools (i.e. EnergyPlus, TRNSYS, IDA-ICE and IES-VE) in predicting the thermal behaviour of one-storey naturally ventilated DSF in three different ventilation modes. To evaluate their capability to predict thermophysical quantities, we compared the simulation results with experimental data. The results show that it is not possible to identify a tool that outperforms the others for all the analysed quantities, especially for the cavity air temperature, which is the least accurate parameter in all software due to underestimation of the daytime peak. IES-VE seems to be most accurate for Supply Air and Thermal Buffer modes when shading is deployed, while EnergyPlus appears most accurate for Outdoor Air Curtain mode. When it comes to surface temperatures and transmitted solar radiation, TRNSYS appears to be the best-performing software. In addition, this study investigated the challenges that designers may face when modelling a naturally ventilated DSF using whole-building simulation tools. Moreover, the investigation elucidates the challenges that have a more significant effect on the performance of the BES tools in order to reinforce their reliability.

1. Introduction

Double skin façades (DSFs) are complex fenestration systems that are designed to actively pursue different building performance objectives, such as thermal and acoustic insulation, ventilation, energy-saving and daylighting. They consist of two parallel transparent façade layers, of single or multiple glazing units, delimiting an air cavity which can offer different ventilation modes between the outdoor and indoor environment, depending on the available openings, while integrating operable solar shading devices. A DSF cavity can be either naturally or mechanically ventilated, and different airpaths can be adopted, depending on the cavity opening configurations and operations: in thermal buffer (TB) mode, it is only operated as a buffer space between the indoor and outdoor; in supply air (SA) and indoor air curtain (IAC) mode, the DSF cavity is used to pre-heat air from the outdoor and indoor environment, respectively, before supplying it to the indoor environment; in outdoor air curtain (OAC) and exhaust air (EA) mode, the DSF is used to reduce the cooling energy needs by exhausting to the outdoor environment the cavity air that entered the cavity from either the outdoor or indoor environment, respectively, thereby removing unwanted solar gains. As far as visual comfort is concerned, the cavity integrated shading device, interacting with the cavity ventilation, can be operated to increase daylight distribution while avoiding glare and overheating. The operational performance of a DSF depends, therefore, on how the different elements are integrated and operated through dedicated control strategies [1,2].

The ventilation in the DSF's cavity is a complex phenomenon, particularly for naturally ventilated cavities, as the temperatures and velocity fields are influenced simultaneously by thermal, optical and fluid-dynamic processes. The airflow in the cavity depends on both wind and buoyancy-driven air movement, which is largely affected by the

* Corresponding author.
E-mail address: fabio.favoino@polito.it (F. Favoino).

https://doi.org/10.1016/j.buildenv.2023.110002
Received 19 September 2022; Received in revised form 16 December 2022; Accepted 9 January 2023
Available online 18 January 2023

Acronym list

BES	building energy simulation
DAQ	data acquisition
DSF	double skin facade
E+	EnergyPlus
EA	exhaust air
ELA	effective leakage area
EMS	energy management system
IAC	indoor air curtain
OAC	outdoor air curtain
MBE	mean bias error
RMSE	root mean squared error
SA	supply air
shOFF	shading is off (up)
shON	shading is on (down)
TB	thermal buffer
TRN	TRNSYS

Nomenclature

ee	External surface of external glazing
ei	Internal surface of external glazing
exh	exhaust
g	solar factor (−)
gap	cavity
ie	External surface of internal glazing
ii	Internal surface of internal glazing
in	Inlet
int	Internal
λ	thermal conductivity of air (W/(m·K))
n	Total number of measurements
out,V	Outdoor vertical
out,H	Outdoor horizontal
ρ_{in}	glazing solar reflectance, inner face (−)
ρ_{out}	glazing solar reflectance, outer face (−)
s	thickness (mm)
S	Irradiance (W/m^2)
τ_{sol}	glazing solar transmittance (−)
T	Temperature (°C)
U	glass thermal transmittance (W/(m^2·K))
U_f	frame thermal transmittance (W/(m^2·K))
X_m	Measured value
X_p	Predicted value

cavity and vent geometries, by the properties of the glazing confining the cavity, and by the properties, geometry, and operations of the shading device. Furthermore, such complex fluid-dynamic phenomena greatly affect the heat exchange within the cavity, thus influencing cavity air and exhaust temperature, cavity and indoor surface temperatures, and long-wave transmitted solar radiation through the DSF towards the indoor environment.

Building Energy Simulation (BES) tools offer the possibility to integrate component-level advanced façade modelling into whole building simulation [3] to study the performance of DSFs under building operation conditions. Nevertheless, just a few of these tools include dedicated modules to model DSF technologies. Thus, modelling workarounds are often necessary. For example, Choi et al. [4] used EnergyPlus to model the operation of a multi-storey natural DSF in TB or SA mode during the heating season. The model was calibrated using experimental data related to the façade temperatures (cavity air, surface temperature of the glazing skins), and the validation results showed good agreement between the predicted and measured values, especially for the inside surface temperature of the inner glazing skin. Khalifa et [5]. investigated the impact of the inner layer composition in a double-skin façade system on the energy loads for conditioning office buildings. The parametric simulation was performed with TRNSYS by varying the glazing type and the glazing area of the inner surface of the naturally ventilated DSF installed on an office building in Tunis (Mediterranean climate). The authors observed that the implications of the various inner skin compositions differ according to the season. For example, double-glazing units reduce the cooling requirements in the hot period by 10%, while single-glazing units perform well in winter.

A series of studies evaluated BES tools' performance [6–9] in simulating DSFs using different methodologies and approaches. However, the accuracy of the different models implemented in the different software tools in describing the dynamic heat and mass transfer processes within DSFs remains largely unknown [10]. This uncertainty is also due to the lack of a homogeneous assessment of the performance of the different software. Notably, there are differences in the use of experimental datasets, façade systems, operational modes, and simulation settings. This greatly reduces the generalisation of the analyses and makes it nearly impossible to compare the performance of the different simulation environments.

This study builds upon previous research [11], where the reliability of four popular BES tools (EnergyPlus, TRNSYS, IDA-ICE and IES-VE, which together cover the vast majority of BES users [12]) in modelling an exhaust-air façade in mechanical ventilation mode (climate façade) was analysed. The present work aims to investigate the performance of the same BES tools in describing the thermal behaviour of a one-storey naturally ventilated DSF, in different airpath modes, by means of experimental validation at façade level. In addition, this work seeks to discuss the challenges that researchers and designers may face when modelling a naturally ventilated DSF using BES tools to reinforce confidence in the performance analysis of buildings integrating such façade systems and highlight directions for model development.

Section 2 presents the main modelling approaches and challenges for naturally ventilated DSFs. Section 3 describes the methodology adopted for the experimental validation and inter-software comparison. Section 4 presents the validation results by comparing main DSF physical quantities from uncalibrated BES models with experimental data. Finally, in Section 5, we reflect on the modelling challenges presented in Section 2 and discuss the impact of specific model parameters.

2. Practices and challenges in modelling naturally ventilated DSFs in BES tools

2.1. Modelling processes

Multiple airflow paths could be adopted in a DSF, and the airflow characteristics depend on the interplay between the outdoor and indoor environmental conditions and the various operational modes. The airflow influences the cavity air temperature profile and the cavity surface temperatures (glass pane temperatures adjacent to the cavity) and is responsible for the convective heat exchange between the cavity and the cavity air. In turn, these variables influence the airflow characteristics, making the problem of simulating the naturally-driven airflow more complex than for DSFs where the airflow is mechanically induced.

Two different approaches exist for modelling DSFs in BES tools (Fig. 1): (i) the "zonal approach", in which thermal and airflow networks are combined to discretise the ventilated cavity in one or more nodes, each corresponding to one zone of the model; (ii) the "in-built component" approach, which consists of a dedicated sub-routine model developed for transparent ventilated façades. In the case of natural

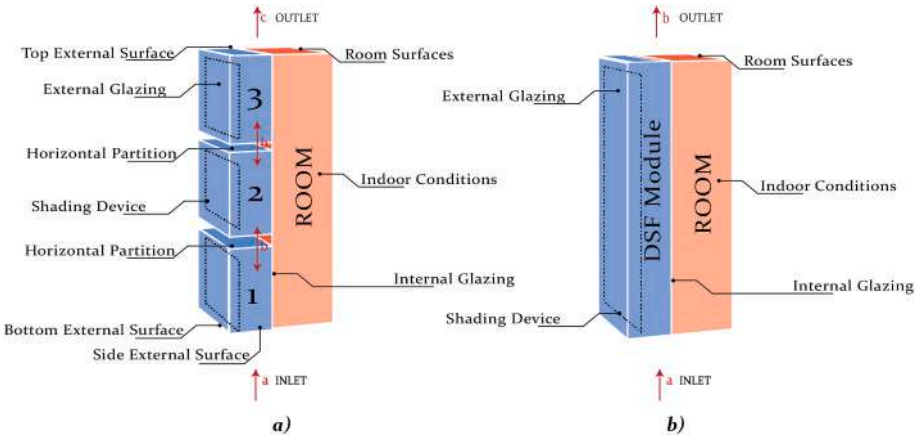

Fig. 1. Zonal (a) versus in-built component (b) approach. Shading device is not drawn for clarity.

ventilation, the zonal approach is the most adopted, especially for multi-storey double-skin façades [13], and it can be implemented in all BES tools by dividing the DSF into several stacked zones linked together to create the airflow network. On the other hand, the in-built component approach can only be implemented in IDA-ICE [14] (among the analysed BES tools) for naturally ventilated DSFs by means of the sub-routine *"Double Glass Façade"*. Similarly, the in-built component models available in EnergyPlus [15] and TRNSYS [16] (*"Airflow Window"* and *"Complex Fenestration System"* module, respectively) can only be used to model mechanically ventilated cavities.

The airflow networks of EnergyPlus and IES-VE [17] are based on the AIRNET model [18], while TRNSYS [19] and IDA-ICE use the COMIS-based model [20]. In all the models, the driving force of the air movement through the airflow network is the pressure difference that occurs due to the combined action of wind pressure and the balance between buoyancy and gravitational forces. While all the models use a general power-law equation to predict flow through cracks and openings, there are differences in the way they deal with the air temperature. In fact, this may change due to heat transfer with the surrounding building fabric (inner and outer skin of the DSF) as the air moves through the cavity. This physical phenomenon affects both the density and viscosity of the air and, consequently, the magnitude of the flow and how this is estimated. Generally speaking, analyses carried out in the past [20] have shown that COMIS and AIRNET lead to similar results in modelling multizone air flows. Thus, there is no ground to assume that one of the two architectures is superior. Different air link components (e.g. cracks, leakage areas, or openings) can be used to link the nodes, each with its mass flow equation as a function of pressure difference, governed by Bernoulli's equation. Based on the relationship between airflow rate and pressure drop for each component, Newton's method is used to solve for the air pressure at each node iteratively until the convergence criteria based on the conservation of air mass flow rate is reached.

The biggest uncertainty in modelling a naturally ventilated DSF in the context of BES tools lies in whether or not the physical-mathematical models adopted to represent airflow and thermal network at the level of the entire building are suitable to represent the physical phenomena occurring in the DSF. In some situations, co-simulation could be technically expedient to solve this problem as it provides an integrated approach to combine different levels and approaches in building simulation by coupling BES tools with component-level models that are based on more detailed physical-mathematical representations [21]. For example, CONTAM [22], a successor of the AIRNET model (as the Airflow Network Model), provides some advantages over EnergyPlus when modelling airflows as it includes a more extensive set of air leakage component models and the ability to define multiple airflow leakage points within a given surface [23]. In the literature, a number of simulation studies of DSF demonstrate the coupling of CONTAM with EnergyPlus [23,24] and TRNSYS [25]. For example, Khalifa et al. [25] applied the co-simulation between TRNSYS and CONTAM to assess the performance in predicting the temperature evolution and the airflow rates into naturally ventilated DSFs, and obtained good agreement between simulation and experimental data using a six nodes airflow network.

When modelling DSFs in BES tools, different modelling assumptions are required, linked both to how to model the façade (i.e., cavity zoning, airflow network design, inlet-outlet opening modelling) and to the type of physical mechanisms occurring inside the ventilated cavity (i.e., wind pressure coefficients, convective heat transfer coefficients, specific heat capacity of glazed systems). Thus, the modelling assumptions are not straightforward, and they became challenges for modellers of naturally ventilated DSFs.

2.2. Modelling assumptions and limitations

Different challenges and intrinsic limitations exist for both approaches (airflow network and in-built component modelling). For the in-built component approach, ad-hoc equations are implemented in the tools able to describe physical phenomena occurring in the ventilated façade. The related parameters and algorithms (e.g., convective heat transfer, solar distribution inside the cavity and pressure drops) are (usually) implemented for a specific type of facade. On the contrary, the zonal approach is more general, as it is meant to model natural air movement throughout the whole building. Nevertheless, DSF parameters for the latter approach are derived and validated at the room (or zone) level, making it more challenging to adopt, as introduced in this section and discussed further in Section 5.

In the zonal approach, the DSF is usually divided into several stacked thermal zones (consisting of the network nodes) linked to the overall thermal and airflow network of the whole building by means of the outlet and/or inlet zones. There is no standardised approach in discretising the number of staked zones, usually ranging from one to six stacked zones for a single-story DSF [12]. In most published studies, the DSF cavity is modelled as three stacked zones per floor [12,26], consisting of the inlet, main cavity and outlet zones. Setting more or less thermal zones to represent the air conditions in the cavity is a choice that usually depends on the complexity of the façade and the desired detail of the outcomes (e.g., the study of the air stratification inside the DSF cavity).

In the zonal approach, the proper design of the airflow network is essential when it comes to modelling a cavity airflow path which connects the cavity to an adjacent zone of the building (e.g. SA, IAC and EA modes) in order to balance the pressure distribution throughout the whole network, as it determines the airflow direction affecting the

facade thermal behaviour. Nevertheless, one of the governing hypotheses of the airflow network in BES tools is that the apertures connecting the airflow nodes are small compared to the space connected (e.g., doors, windows and louvres), which poorly approximates the conditions of a DSF, where the characteristic size of the opening is of the same magnitude as the cavity section, and thus distributed pressure losses along the cavity cannot be considered as negligible. Therefore, in order to achieve a good model formulation, it is necessary to make appropriate adjustments, such as adding narrowings along the cavity in order to distribute pressure losses throughout the cavity or adopting a fictitious airflow resistance due to the obstruction in the cavity, such as shading devices.

The driving forces of the airflow network are the natural stack effect and wind pressure. All BES tools allow the user to define the different surface averaged pressure coefficients to calculate the wind pressure on the different external surfaces by implementing Bernoulli's formulation described in the ASHRAE Fundamentals (2001) [27]. The wind pressure coefficients may be obtained by various means (measurements, CFD studies and wind tunnel experiments), though the modeller does not have access to these data in most cases. Thus, generally, the coefficients employed in the calculations are the ones available in the tool adopted: Energy Plus and TRNSYS refer to ASHRAE Fundamentals values, while IDA-ICE and IES-VE refer to the results of the wind tunnel experiment from the AIVC publication [28]. Except for IES-VE, the tools differentiate the coefficients according to the exposure type (exposed, semi-exposed and sheltered), while IES-VE also takes into account the geometry of the building (low-rise, high rise) and the building surface (short or long wall).

The inlet and outlet openings of the DSF are considered an obstacle to the free movement of the air, and are therefore seen as creating a pressure drop. Additionally, in large openings, the airflow has a vertical velocity profile, which depends on the different air densities as a function of the height. It is best practice in BES tools to use non-linear equations to calculate the flow as a function of the pressure difference through the openings, depending on the opening geometry. Small openings are modelled by the Effective Leakage Area (ELA) or the crack method. The ELA method is implemented in EnergyPlus and IDA-ICE (where both approaches are available), and the complexity of using this method is the estimation of the ELA value to employ. The leakage area values available in the ASHRAE Fundamental for different building component types [29] refer only to a few standard window typologies and do not fit the openings usually installed in a DSF. The latter is also used to model the air infiltration due to the airtightness of the openings; thus, the modeller is required to insert the mass flow and exponent coefficient, which are usually unknown and are not easily found in the literature [10]. More complex formulations considering the airflow in both directions are used for large openings. In all tools, they are treated as sharp-edged orifices, where the mass flow is a function of the equivalent orifice area of the opening and its discharge coefficient. In most tools, the responsibility to define this correlation is left to the modeller, while TRNSYS and IES-VE implement correlations for several opening typologies (sliding doors, side, top and bottom hinged windows). Conversely, most tools allow the definition of the discharge coefficient freely, while in IES-VE, this is fixed to 0.62. Nevertheless, these models were developed to evaluate natural ventilation in buildings and are therefore validated for standard components (e.g., doors and windows) and not for specific ones such as ventilation openings of DSFs.

In the cavity, different heat flow patterns will occur with changing temperatures and varying positions of the ventilation openings and solar shading (e.g., blind slats angle). From the thermal network point of view, the convective heat exchange process between airflow and glass panes enclosing the cavity and between airflow and solar shading surface (if any) is exceedingly difficult to model correctly [10]. EnergyPlus offers a selection of different methods to calculate the interior heat transfer coefficient. The most widely used method is the "adaptive algorithm", which chooses the correct correlation for the convective coefficients based on the classification of surfaces and the flow regime. In the natural regime, the coefficient is calculated according to the Standard ISO 15099 [30]. In TRNSYS, it is possible to choose between variable coefficients derived from empirical equations (provided by the user) or the internal calculation method, which uses the ASHRAE Vertical Wall algorithm, whereas IES-VE adopts Alamdari and Hammond's correlation [31]. As for previous parameters (concentrated and distributed pressure losses), these correlations were developed and validated for room conditions, where the effects of the other surfaces' temperature are negligible and do not impact the flow of the analysed surface. In DSFs, however, the aspect ratio of the cavity section is orders of magnitude different than room geometries (even more so when the shading is present in the cavity). Therefore, replicating the physical behaviour of DSF cavities may require different empirical correlations than those used to model convective heat and mass transfer for conventional rooms.

Cavity shading is usually assigned to one of the two glazing systems of the DSF, as an internal or external shading device, and only the part of the cavity between the shading and the corresponding glazing layer is considered ventilated. Convective heat exchange coefficients for shading devices are also usually derived from configurations with geometrical features and thermal gradient fields far from those seen in a DSF (i.e., internal blinds), potentially leading to inaccuracy in predicting how heat is released to the cavity airflow from the shading device.

Finally, the thermal mass of the materials is usually considered when modelling opaque envelopes but not when modelling glazed ones. This legacy originated when glazed surfaces were often limited in size and weight (e.g., with single-glass panes). However, DSFs are multi-layered glazed structures that usually cover large façade areas and adopt rather thick glass panes for safety and structural reasons. The combination of these two conditions leads to the fact that the inertial features of DSFs might not be negligible, especially when it comes to the prediction of the temperature of the indoor-facing surface of the inner skin. With the exception of IDA-ICE, the analysed tools do not consider the thermal mass of the glazing system [12].

3. Methodology

In this section, the characteristics of the DSF mock-up used for the validation are presented together with the related experimental campaign, and the methodology followed for the model validation. In addition, how the DSF was modelled in the different BES tools is briefly discussed, leaving the details of each DSF model for a specific BES tool in Appendix A, for the sake of readability.

3.1. Case study DSF and experimental campaign

The DSF mock-up is a single-story facade developed to modulate to the maximum extent the overall heat transfer between the indoor and outdoor environment. It consists of two parallel transparent skins with an aluminium framing system as schematised in Fig. 2. Both inner and outer skins present an equally sized (1.22 m width and 2.00 m high) double glazing unit made of a 6 mm outer clear glass pane, a 16 mm cavity filled with a gas mixture of air and Argon at 90% and a 6 mm inner clear glass plane, with low-E coating on surface 3 and 2, the inner and outer surface of the cavity respectively (cf. Fig. 2 for details of the thermal and optical properties of the DSF components). The parallel skins form a 250 mm thick ventilated air cavity containing a controllable light grey roller curtain located at the centre of the cavity. Four pivoted opaque ventilation openings (1.5 m × 0.5 m) are placed on the inner (bottom and top) and outer (bottom and top) skin, controlled by its linear actuator (openable up to 45°). Thus, this prototype can adopt all the possible airpath configurations achievable by a DSF (cf. Fig. 2): Thermal Buffer (TB, all vents closed), Outdoor Air Curtain (OAC, vent 1 and 2 open), Supply Air (SA, vent 1 and 3 open), Exhaust Air (EA, vent 4 and 2 open), and Indoor Air Curtain (IAC, vent 4 and 3 open).

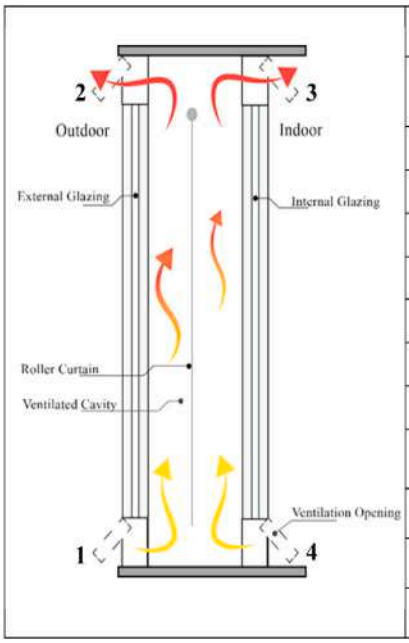

	Ext.Glazing	Shading	Cavity	Int. Glazing
Type	Double glazing – lowE inner glass	Roller curtain	Ventilated	Double glazing – lowE inner glass
s [mm]	29	1	250	29
τ_{sol} [-]	0.55	0.03	-	0.55
ρ_{out} [-]	0.20	0.30	-	0.20
ρ_{in} [-]	0.07	0.30	-	0.07
U [W/m²K]	1.21	-	-	1.21
g [-]	0.58	-	-	0.58
U_f [W/m²K]	1.50	-	-	1.50
1 Outdoor inlet **2** Outdoor outlet **3** Indoor outlet **4** Indoor inlet				
1→2	Outdoor Air Curtain - **OAC**		**1→3**	Supply Air - **SA**
4→3	Indoor Air Curtain - **IAC**		**4→2**	Exhaust Air - **EA**
All openings closed			Thermal Buffer - **TB**	

Fig. 2. Schematic section and physical properties of the double skin façade prototype.

The DSF prototype was installed in the south-exposed facade of the TWINS (Testing Window INnovative Systems) outdoor test cell facility of the Polytechnic University of Turin (45 N° latitude 7.4° E longitude), where the monitoring campaign was carried out for several months to fully characterise the performance of the DSF in different airpath configurations and under different boundary condition. The monitoring system acquired the following quantities (Fig. 3): temperatures inside the DSF cavity (one at the inlet, one at the outlet and four at different heights inside the cavity); indoor and outdoor air temperatures; inner and outer surface temperature values for each glazing (2 for each side); test cell average surface temperatures; air speed inside the cavity (at different heights); total vertical solar radiation incident on and transmitted through the facade. Weather data were recorded by integrating the campus weather station (nearby the outdoor test facility) and the local one logging outdoor dry-bulb air temperature and relative humidity, atmospheric pressure, global horizontal solar irradiance, wind velocity and direction.

Measuring air speed in naturally ventilated cavities for continuous monitoring is still challenging [32], and within this campaign, the measuring range was, most of the time, of the same order of magnitude as the accuracy of the hot-wire anemometers; therefore, we decided to exclude this variable in the validation study. Moreover, best practices established in the literature were adopted to reduce the influence of solar irradiance on the measurement of temperature physical quantities [33,34]. Due to the cones adopted to shield the pyranometers from internal reflections, which may reduce the accuracy of the measurements in the early morning and late afternoon, it was decided to filter the irradiances to calculate model performance indicators for this variable by considering only the central hours of the day (from 11:00 to 15:00).

After calibration and verification, the accuracy of the entire measurement chain linked to façade-level physical quantities was: ±0.5 °C for thermocouples, ±0.3 °C for thermal resistances and ±5% for pyranometers.

During the monitoring campaign, the DSF mock-up was operated with different air paths and shading device configurations (positions and types). For validation purposes, it is interesting to investigate the performance of software prediction in the most heterogeneous conditions – in terms of boundary conditions (seasonality, sunny and cloudy days, warm and cold days) and façade configurations. Based on these considerations, three ventilation paths – thermal buffer (TB), outdoor air curtain (OAC), and supply air (SA) – were selected and combined with two shading states; roller screen in position up and down. TB refers to the façade configuration where all the ventilation openings are closed, and there is no mass exchange between the cavity and the surrounding environments. In both OAC and SA, outdoor air enters the cavity but is released towards the outside (OAC) or the inside of the test cell (SA). Fig. 4 displays the boundary conditions (outdoor and indoor air temperatures and global horizontal irradiance) for each configuration; the chosen representative day for the analysis of each dataset is highlighted with a grey background. The cell's indoor air temperature setpoint was set to 20 °C in winter (for SA and TB modes) and 26 °C in summer (OAC mode).

3.2. DSF model implementation and simulation in BES tools

The primary purpose of this investigation was to compare the performance of the different BES tools to replicate the thermophysical behaviour of a single-story naturally ventilated cavity. For this reason, the evaluation was focused on the physical quantities related to the DSF and not on the room-level physical quantities (e.g., indoor air temperature). The internal zone of the test cell was modelled as a simple box whose construction features and equipment quantities (indoor air temperature, walls' stratigraphy and energy needed for heating or cooling) were not of interest to the analysis and therefore were provided as boundary conditions for each software. For this reason, in all the BES tools, the indoor air temperature and surface temperature of zone opaque components were imposed through schedules created using the available experimental data to eliminate the uncertainty due to the internal zone and focus the validation procedure solely on the thermal and airflow network representing the DSF. For this validation study, it was decided to use un-calibrated models. Thus, all available information about the mock-up was inserted into the models and the default values were used for unknown information. In this study, priority was given to the in-built component module over the zonal approach, if available in the tool, as a modeller would use the dedicated module (if any) compared to a more complex modelling task required for the zonal approach. Therefore, the in-built component approach was chosen for IDA-ICE, while the zonal approach was used for the other tools.

In the zonal approach, the DSF cavity was modelled as three stacked thermal zones corresponding to the inlet, the cavity, and the outlet zone.

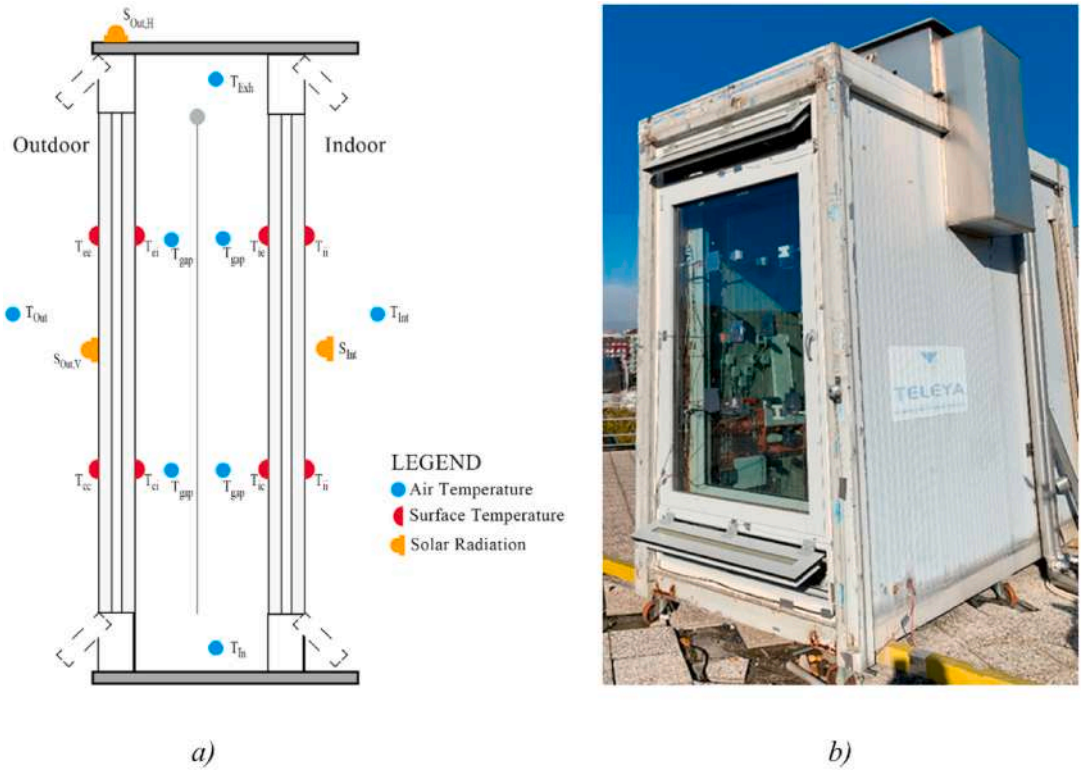

Fig. 3. Sensors scheme (a) and picture of flexible DSF prototype in OAC mode and shading up (b).

Only the cavity zone contains the glazing systems, and its volume is four times the volume of the adjacent stacked zones, while the openings towards indoor and outdoor are placed on the inlet and outlet zones. This allowed us to have model outputs in line with the physical quantities available in the experimental dataset. When modelling the SA mode for the zonal approach, to ensure an overall airflow amount and direction (from the outside, to the DSF cavity, and finally to the adjacent zone) in line with the experimental data, it was necessary to extend the DSF airflow network to the internal zone and to add a fictitious duct connecting the volume of the test cell to the outdoor representing the test cell leaks to the outdoor (1 m high, cross-section of 0.1 m^2).

A customised weather data file with a standard time resolution of 1 h was generated based on the data gathered from the outdoor weather station[1] for the six periods (cf. Fig. 4). The simulation time-step in each tool was set to 10 min, and the numerical output was extracted with a resolution time of 1 h. The variety of the outcomes related to the façade – in terms of the cavity air, surface temperatures, and solar irradiance - depends on the modelling approach adopted by each software. Usually, the component model provides less output information than the zonal model. For example, the "*Double Glass Façade*" component of IDA-ICE calculates a unique temperature for the whole cavity, and it is not possible to extract the cavity outlet air temperature. On the other hand, it is possible to obtain more information and outputs, such as the air temperature stratification along the cavity through the zonal approach. Moreover, dedicated postprocessing of the simulation outputs was carried out to obtain the total transmitted solar radiation by the DSF in EnergyPlus and IES-VE, as detailed in Appendix A. Table 1 summarises the settings of the simulation condition and DSF modelling approach used for each BES tool. Detailed information on DSF model implementation for each BES tool is reported in Appendix A.

3.3. *Validation* ***procedure***

The validation of the different BES tools is based on the comparison of the three physical quantities[2] reflecting the influence of the DSF on the heat balance of the thermal zone adjacent to the facade:

- the temperature of the air in the DSF cavity [°C];
- the temperature of the interior surface of the inner skin [°C];
- the transmitted solar irradiance through the façade [W/m^2];

The performance of each software was analysed qualitatively through a scatter plot that compares the experimental data with the predicted outcomes of the software. In addition, the time profile of one representative day for each configuration was compared with the experimental data to better understand the aggregated results and detect any particular deviations of trends during the day.

Two statistical indicators were used to compare the fitness of the prediction with the experimental data quantitatively: the Mean Bias Error (MBE) and the Root Mean Square Error (RMSE):

$$MBE = \frac{1}{n}\sum_{i=1}^{n}\left(X_p - X_m\right)_i \quad (1)$$

$$RMSE = \sqrt{\frac{1}{n}\bullet\sum_{i=1}^{n}\left(X_p - X_m\right)_i^2} \quad (2)$$

[1] the quantities directly utilised to customise the weather file were outdoor dry bulb air temperature, relative humidity, atmospheric pressure and global solar irradiance. The latter was decomposed in the normal beam and diffuse global solar irradiance, calculated using the ENGERER2 separation model [39], and the cloudiness factor was taken from the climate reanalysis ERA5 [40]. This solar decomposition was validated by comparing the calculated vertical global solar irradiance on the South façade with the measured value.

[2] Since all the tested BES tools provide a unique output value, volume and area weighted average were calculated for the experimental temperature of the air in the cavity and the temperature of the inner skin's surface, respectively.

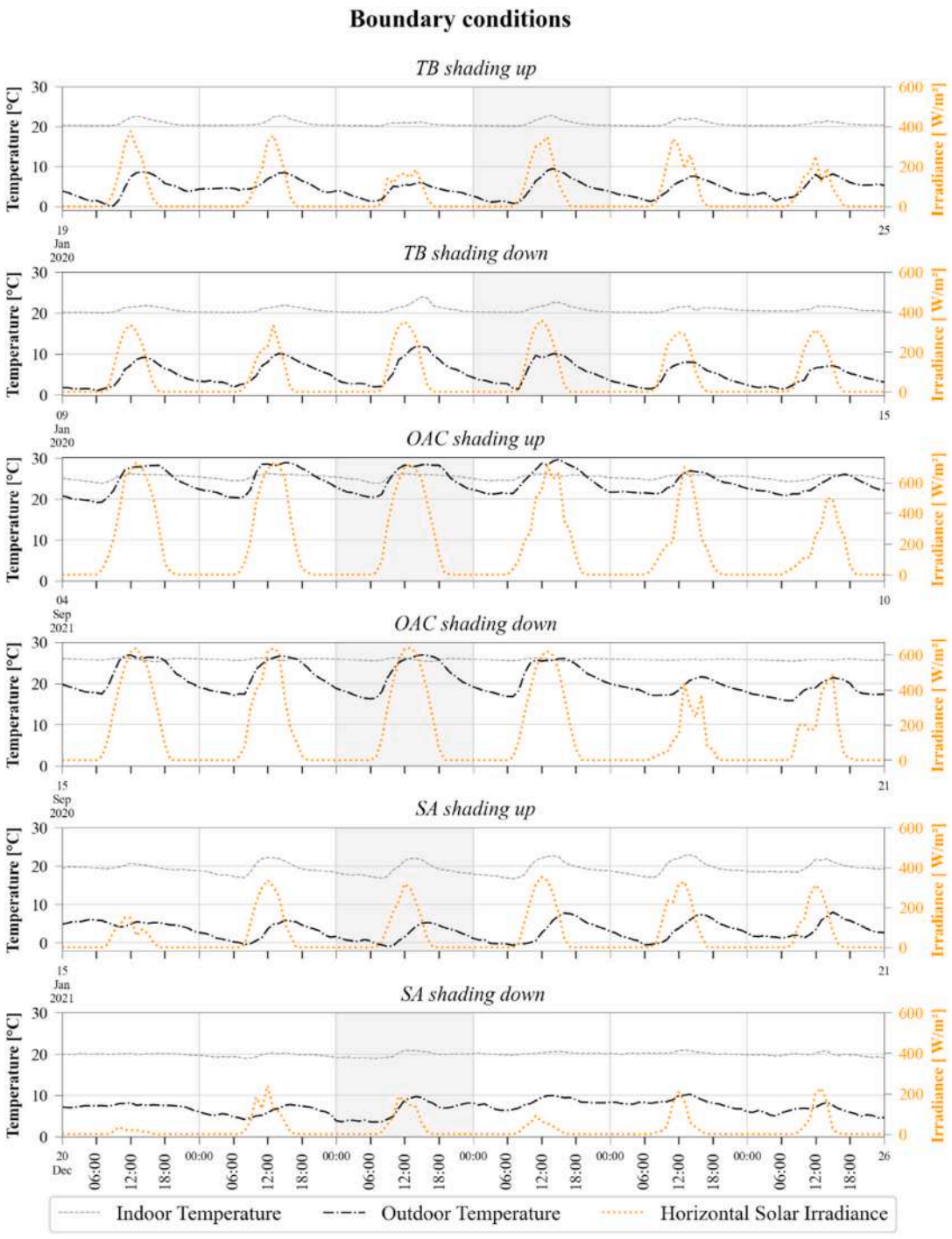

Fig. 4. Time profile of indoor air temperature, outdoor air temperature and horizontal solar irradiance during the six periods. The representative day for each dataset is highlighted in grey.

The MBE provides the average bias of the prediction, and positive values indicate an overall overestimation of the prediction; in contrast, negative values indicate model under-prediction. However, the main drawback of this indicator is that it is subject to error compensation due to the sum of positive and negative values. For this reason, the RMSE index was calculated; it returns the standard deviation of the prediction errors but loses the information on the sign (under- or over-estimation).

It is important to highlight that while threshold values for MBE or RMSE to consider a model validated can be found for whole building models [35], for component-level validation, there are no established maximum values not to be exceeded for any quantitative indicators to consider the model "validated". In the context of the study, we, therefore, use values of the statistical indicators in combination with a qualitative analysis of the results (e.g., time and intensity match between the simulated and experimental hourly profile) to assess the validity of the predictions of each BES tool.

4. Results

The results of the validation study are presented in two main sections.

Firstly, the performance of each BES tool is presented (Section 4.1 to

Table 1
Settings of simulation condition and DSF modelling approach used for each BES tool.

		EnergyPlus	TRNSYS	IDA ICE	IES-VE
Simulation conditions	Exterior convective surface algoritm	SimpleCombined [15]	Vertical window's internal algorithm [19]	Clarks [12]	McAdams [12]
	Interior convective surface algorithm	AdaptiveConvectionAlgorithm [15]	Vertical window's internal algorithm [19]	*Default*[a] max(Table, CDA) [12]	Alamdari & Hammond [31]
	Solar distribution	FullInteriorAndExteriorWithReflections [15]	Detailed radiation model [19]	*Default*[a]	*Default*[a]
	Temperature set-point	Ideal load	Ideal load	Ideal load	HVAC
	Timestep for heat balance	10 min	10 min	*Default*[a] Adaptive	10 min
DSF Modelling approach	Cavity modelling	Zonal approach	Zonal approach	Component model	Zonal approach
	Horizontal partition	Horizontal opening - infrared transparent material	Always-opened large windows	n.a.	Always-opened large windows
	Ventilation openings	Pivoted window	Large pivoted window	Default[a] Leaks (ELA)	Large openings ('*Top - Hung*' category) [17]
	Shading device	Interior shading of the exterior window	Interior shading of the exterior window	Interior shading of the exterior window	Interior shading of the exterior window
	Wind exposure	City	*Default*[a]	Semi-exposed	Semi-exposed low-rise
	Specific heat capacity	n.a.	n.a	Present	n.a.
	Air Mass Flow Coefficient C_{MF} (for closed vents)[b]	0.002 kg/(s·m· $Pa^{0.7}$)	0.002 kg/(s·m· $Pa^{0.7}$)	0.0001 m^2[c]	0.015 l/(s·m· $Pa^{0.6}$)
	Air Mass Flow Exponent n (for vents closed)[b]	0.7	0.7	0.5	*Default*[a] 0.6

[a] Default settings.
[b] When vents are closed, the following power law form (crack flow) is used $Q = C_{MF} \cdot (\Delta P)^n$
[c] ELA method applied [equivalent leakage area at $\Delta P = 4$ Pa ($C_d = 1$)].

4.4) for the prediction of the three physical quantities (cavity air temperature, internal surface temperature, and transmitted solar radiation) in the three air-path configurations (TB, SA and OAC) using scatter plots of simulation output vs experimental data for six days of continuous monitoring (cf. Fig. 4). In each scatterplot summarising the results, from top to bottom, the cavity air temperature (Figs. 5, 6, 7 and 8a), the surface temperature (Figs. 5, 6, 7 and 8b) and the transmitted solar irradiance (Figs. 5, 6, 7 and 8c) are represented for the three air-path configurations (from left to right) in TB, OAC and SA mode. The different curtain shading modes are combined in the same scatterplot.

Then, the time profile of each specific physical quantity of interest (Figs. 9–11) for the different software tools was compared in an inter-software comparison and against experimental data (Section 4.5) for typical days (cf. Fig. 4, grey background), in addition to the scatterplot distribution and error boxplot (including all DSF operational modes and blind configurations together).

4.1. Energy Plus

EnergyPlus showed different performance in the prediction of the cavity air temperature for the different air paths, and this was likely due to the challenges of the Airflow Network to predict the direction of the airflow accurately (Fig. 5): when there is no interaction with the indoor zone (OAC and TB modes), the software exhibited satisfactory performance in the prediction of the cavity air temperature, whereas this quantity was systematically overestimated with an average $RMSE_{E+,SA} = 10.3$ °C for the SA mode (Table 2). To improve the performance of the tool in predicting the cavity air temperature in SA mode, a co-simulation strategy with CONTAM was explored. This approach achieved a significant improvement (Fig. 5.a, right) as all the data points were well distributed among the scatter plot's bisector, albeit with some underestimation outliers (peak values of the cavity air temperature when the shading is raised). Conversely, for OAC mode (Fig. 5, middle), the points were well distributed among the bisector even without the need to implement a co-simulation scheme with CONTAM, showing an elevated performance level in the prediction of the cavity air temperature. For TB mode, a slight underestimation for high temperature and an overestimation for low temperature was seen (Fig. 5, left). The surface temperature exhibited the same trend as the cavity air temperature: the prediction was highly accurate at night, while the magnitude of the peaks was generally underestimated – and this became especially relevant when the curtain was raised. Moreover, for the SA mode, the use of CONTAM resulted in an improved surface temperature prediction, showing that the airflow significantly influenced the temperature distribution in the glazing system (Fig. 5b, right).

Finally, the tool significantly underestimated the total transmitted solar irradiance, as visible from Fig. 5c (cf. Table 4, $RMSE_{OAC} = 81.3$ W/m^2, $RMSE_{SA} = 82.5$ W/m^2).

4.2. TRNSYS

The cavity air and surface temperature predictions (Fig. 6a and Fig. 6b) exhibit a good fit with experimental data, especially for the outdoor air curtain and supply air modes. It is possible to notice that the fitness of the model is better in the low-temperature range, and the points begin to diverge from the bisector for temperatures greater than 30 °C. For the thermal buffer mode, the points were still well distributed along the bisector (with low MBE), but with a wide distribution (high RMSE), especially for the high-temperature range (Fig. 6a and Fig. 6.b, left). As for EnergyPlus, not considering the thermal mass of the glazing systems affected the prediction of the surface temperatures in TB ($RMSE_{TB,\ shON} = 2.2$ °C, Table 2) compared to when the cavity was ventilated, as visible in the SA mode (Fig. 6b) even though some outliers are present in the low-temperature range; in OAC mode the points followed an irregular trend due to an underestimation of surface temperature in the mid-range. Finally, TRNSYS exhibited excellent performance predicting the solar irradiance transmitted through the double skin façade (Fig. 6c), both in configurations with the solar shading raised and deployed (cf. Table 4, $RMSE_{max} = 38.7$ W/m^2).

4.3. IDA-ICE

Unlike with the other BES tools, the in-built DSF component model was used within IDA-ICE. In general, the tool was able to predict the dynamics of thermal behaviour, but the accuracy in the prediction of the magnitudes was lower, especially for high temperatures. Even though it is the only software to include the capacitive node in the window models and provides the dedicated module with the ventilated cavities, the

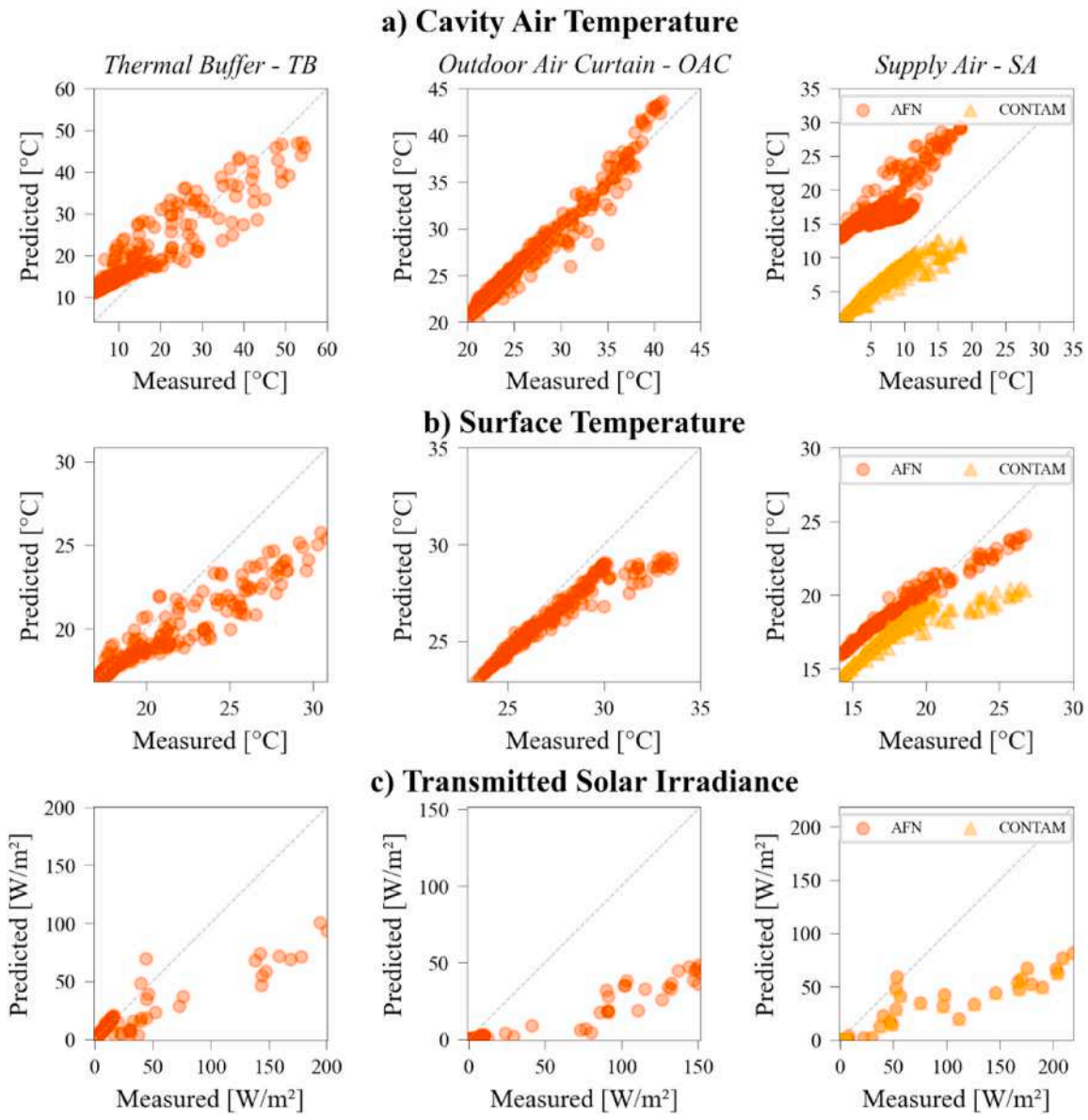

Fig. 5. Comparison between experimental data and predicted outcomes carried out with Energy Plus. From top to bottom: Cavity air temperature, Surface Temperature, Transmitted Solar Irradiance. From left to right: Thermal Buffer, Outdoor Air Curtain and Supply Air.

comparison of the outcomes with the experimental data of the cavity air temperature (Fig. 7a) and surface temperature (Fig. 7b) was not very satisfactory. In the case of the configurations with ventilation in the cavity (OAC and SA modes), the software underestimated the peak with an average error of 10 °C, although the prediction error was drastically reduced at night-time. Conversely, in TB mode the trend of the cavity air temperature was in phase with the measured data and the peak was accurately predicted, whilst higher errors were measured for the cavity air temperature at night time, thereby reducing the performance of the statistical indices ($RMSE_{TB,\ shOFF} = 3.16$ °C, $RMSE_{TB,\ shON} = 4.1$ °C). As far as the time profile of surface temperatures (Fig. 7b) is concerned, for OAC and SA mode, with and without shading, the peak was consistently underestimated, but the prediction error drastically reduced at night time. Additionally, the transmitted solar radiation was accurately predicted (Fig. 7c), with a certain underestimation of the peak when the shading was not present in the cavity, which, nevertheless, did not impair the overall prediction of the shortwave radiative heat transfer across the DSF.

4.4. IES-VE

As far as the prediction of the cavity air temperature is concerned, IES-VE exhibited a varying performance for different ventilation modes: in TB configuration (Fig. 8.a, left), the software tended to overestimate the peak (especially in the absence of the shading) and to anticipate it with respect to the measured data; when the cavity was ventilated in OAC mode (Fig. 8.a, center), the tool underestimated the peak, reducing such difference in the absence of solar radiation; in SA mode the performance of the prediction of the cavity air was improved, especially when the roller shade was deployed (Fig. 8.a, right). The surface temperature prediction (Fig. 8b) followed the trend of the cavity air temperature. As for EnergyPlus and TRNSYS, this is due to the model neglecting the thermal mass of the glazing. Therefore, the peak value was always underestimated and anticipated, especially for the TB mode. The prediction of the solar radiation transmitted by the façade was under-estimated when the shading was raised, and it had an excellent fit in the presence of roller shading in the cavity (Fig. 8c), which could be due to inaccurate distribution of the solar beam radiation between two

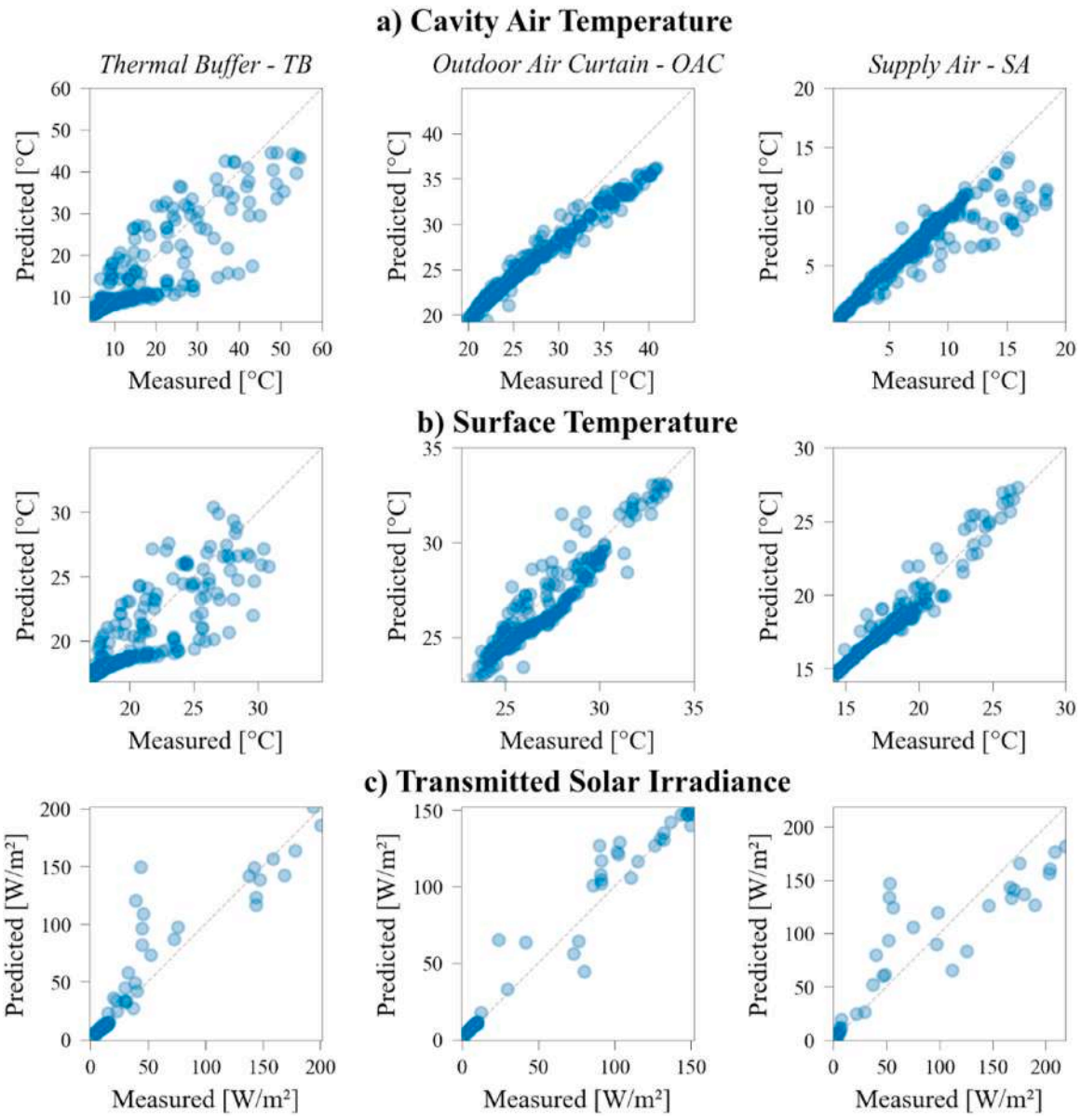

Fig. 6. Comparison between experimental data and predicted outcomes carried out with TRNSYS. From top to bottom: Cavity air temperature, Surface Temperature, Transmitted Solar Irradiance. From left to right: Thermal Buffer, Outdoor Air Curtain and Supply Air. The shading configurations are combined.

Table 2
MBE and RMSE values of the cavity air temperature calculated for the six DSF configurations.

	Cavity air Temperature [°C]											
	Thermal Buffer				Outdoor Air Curtain				Supply Air			
	MBE		RMSE		MBE		RMSE		MBE		RMSE	
Shading	down	up	down	up	down	up	down	up	down	up	down	up
EnergyPlus	3.3	5.8	7.0	6.5	0.6	0.3	1.4	0.9	−0.6	−1.0	0.9	2.4
TRNSYS	−2.1	0.7	7.3	3.9	−1.4	−1.2	2.0	1.8	−0.5	−1.5	0.7	2.7
IDA ICE	0.0	2.4	4.1	3.2	−1.9	−1.6	3.2	2.4	0.5	−0.1	0.7	2.1
IES VE	2.8	4.0	6.8	5.2	−2.3	−1.6	3.7	2.5	0.9	0.5	1.0	1.7

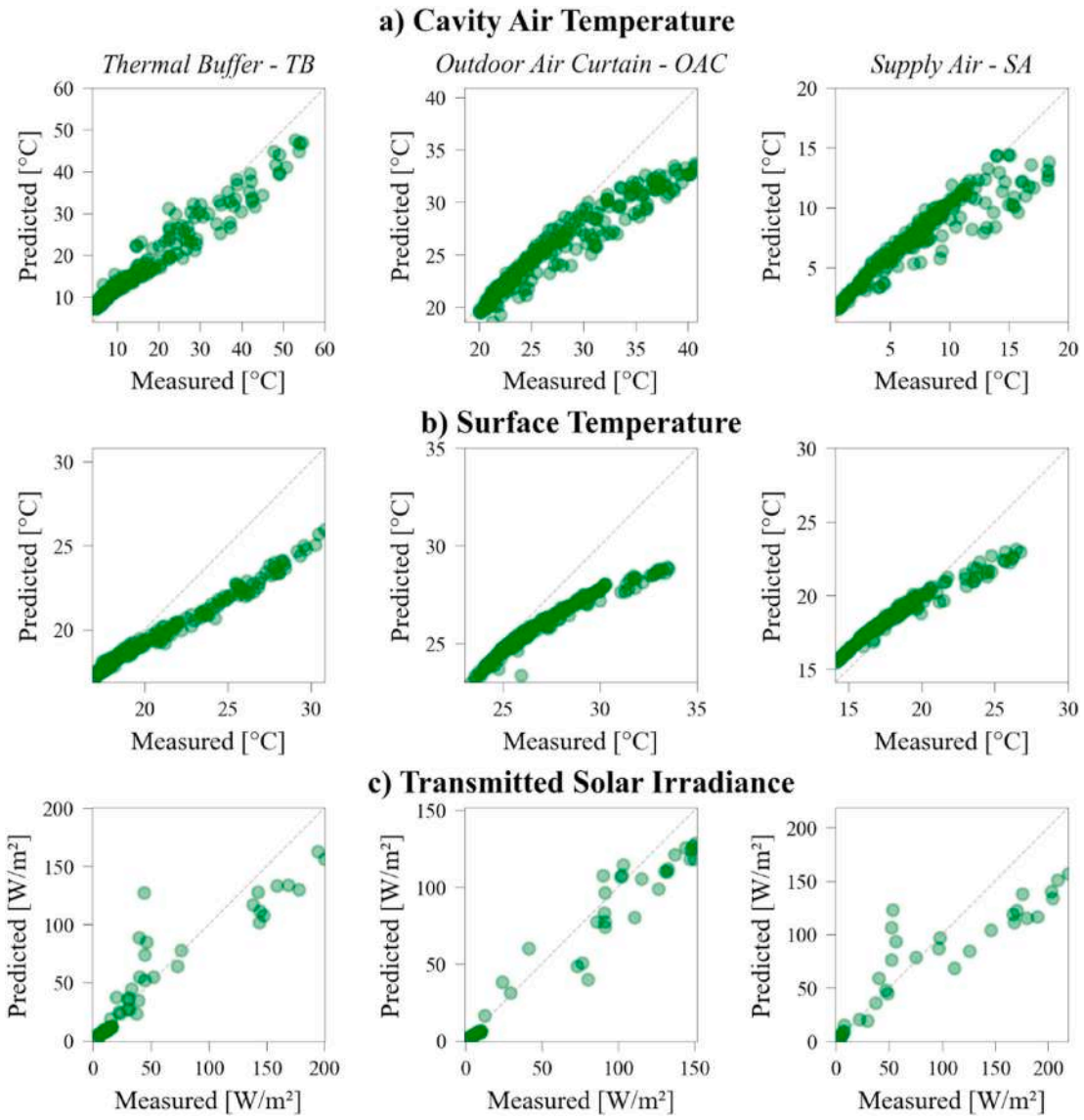

Fig. 7. Comparison between experimental data and predicted outcomes carried out with IDA-ICE. From top to bottom: Cavity air gap temperature, Surface Temperature, Transmitted Solar Irradiance. From left to right: Thermal Buffer, Outdoor Air Curtain and Supply Air. The shading configurations are combined.

internal zones.

4.5. Inter-software comparison

The errors in the prediction of the cavity air temperature for each BES tool are shown in Fig. 9. Under the OAC mode, the prediction of the four tools was quite similar in both states of shading: with the exception of EnergyPlus, the peak values during the day were significantly underpredicted, whereas all trends overlapped very well with the experimental data during the night. The statistical indicators reported in Table 2 reveal that EnergyPlus was the most accurate software for predicting the cavity air temperature for modelling the OAC mode ($RMSE_{E+,shOFF} = 0.9$ °C, $RMSE_{E+,shON} = 1.4$ °C), whereas all other tools were significantly more inaccurate, especially for IES-VE and IDA-ICE when the shading is raised. The overestimation of the mass flow rate in the cavity in TRNSYS, IES-VE and IDA-ICE was greater compared to EnergyPlus (which was the best tool in this case, as mentioned before), reducing the peak of temperature during the daytime. Unfortunately, we cannot use experimental air velocity data to support this assumption.

IES-VE is the tool that best predicted the cavity air temperature for SA mode, as quantified by the statistical indicators of Table 2 and the time series in Fig. 9. Moreover, the performance of the four BES tools was quite similar when the shading is deployed. It is noteworthy that the SA mode requires the integration of the DSF airflow network into the whole building network to balance the pressure distribution properly. However, EnergyPlus failed to predict the cavity air temperature. Comparing the outcomes of EnergyPlus in terms of the cavity air and indoor air temperatures, it appears that the predominant airflow direction was clearly from the room zone to DSF and not vice versa. Using any available connectors among the possible AirflowNetwork components (e.g. cracks, leakage areas, or large openings), it was not possible in EnergyPlus to ensure a flowrate that proceeded smoothly from the outdoor to the DSF cavity and then further to the test cell zone. The co-simulation with CONTAM fixed this issue, as visible from the statistical errors, comparable with the other software (cf. Table 2).

In TB mode, it is possible to observe that TRNSYS, EnergyPlus and IES-VE predicted the cavity air peak values approximately 1 h beforehand compared to experimental data for both shading configurations. This time shift was less evident from IDA-ICE simulation outputs. Since the boundary condition profiles (solar irradiance and outdoor air temperature) were in phase, the time lag was likely due to the absence of information about the heat capacity of the glazed layers in the models of

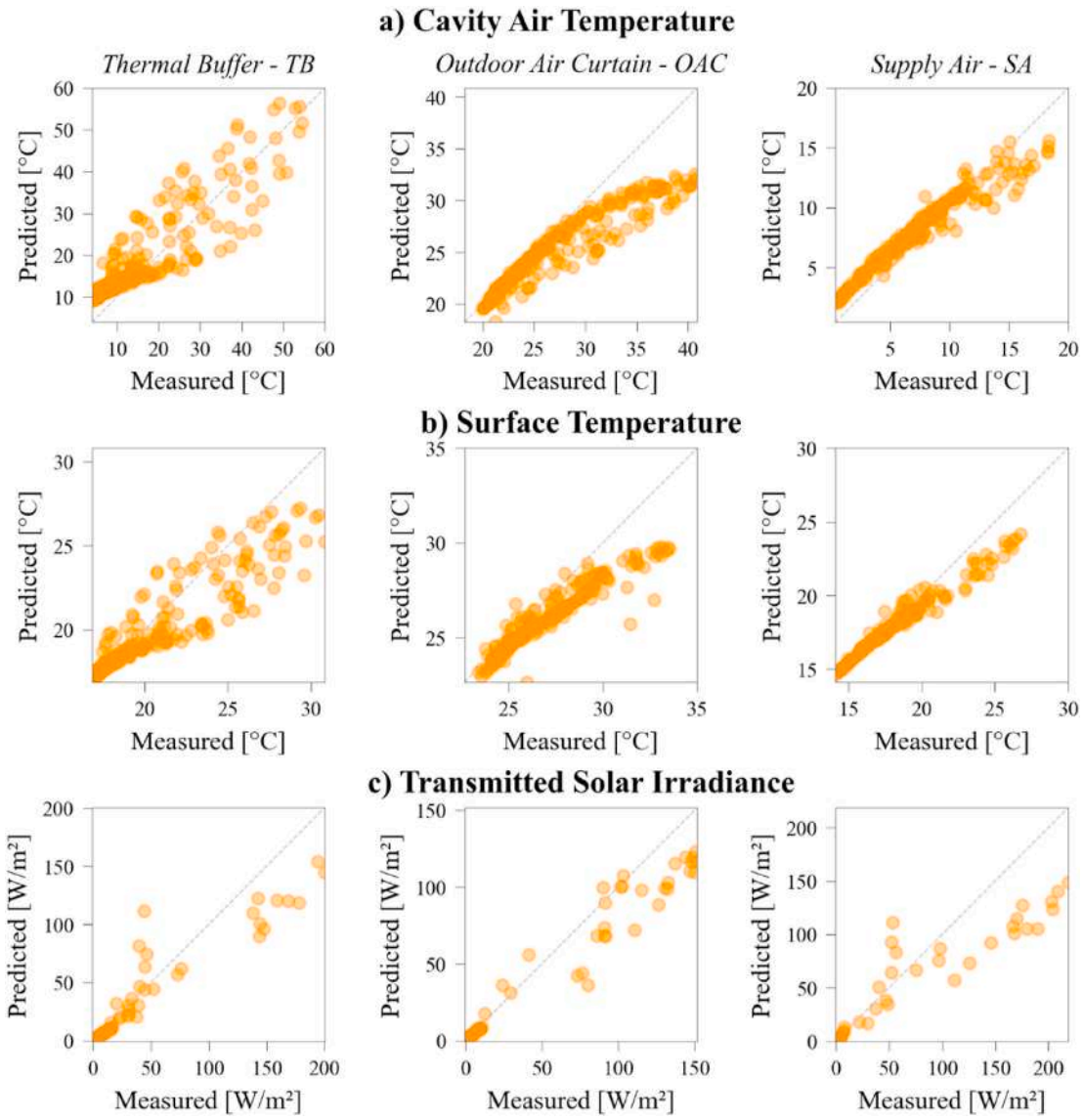

Fig. 8. Comparison between experimental data and predicted outcomes carried out with IES-VE. From top to bottom: Cavity air temperature, Surface Temperature, Transmitted Solar Irradiance. From left to right: Thermal Buffer, Outdoor Air Curtain and Supply Air. The shading configurations are combined.

the transparent components for the three BES tools. With this simplification, the software tools do not correctly model the dynamics of the absorption and reemission by the glazing systems of the solar irradiance, resulting in a delay of the temperature peaks. In TB mode, these effects are more pronounced since mass exchange between the DSF cavity and surrounding zones is minimal - hence the heat transfer from the envelope system to the air in the cavity is the driving force that determines the cavity air temperature. This effect was pronounced when the roller shade is deployed, as the peak underestimation was increased by absorbed solar radiation transferred from the shading to the air cavity by means of convection. For the other ventilation modes, TRNSYS, EnergyPlus and IDA-ICE tended to underpredict the peak cavity temperature when the shading is deployed, whilst the performance of IES-VE was unaltered.

The prediction of the indoor surface temperature of the inner skin of the DSF is shown in Fig. 10. Overall, TRNSYS and IES-VE were the best-performing tools in predicting inner glazing surface temperatures, depending on the ventilation mode. As shown in Table 3, IES-VE was the best-performing tool in predicting the surface temperature in TB mode and both shading modes. TRNSYS, in contrast, had the lowest statistical errors in OAC and SA modes. In particular, in SA mode with shading deployed, the performance of all software was quite similar (cf. Table 3).

EnergyPlus TRNSYS and IES-VE predicted the peaks about 1 h ahead of the measurement data, following a similar trend as for the cavity air temperature. In contrast, IDA-ICE provided a better time match between simulation and experiments due to the inertial features of the glazing

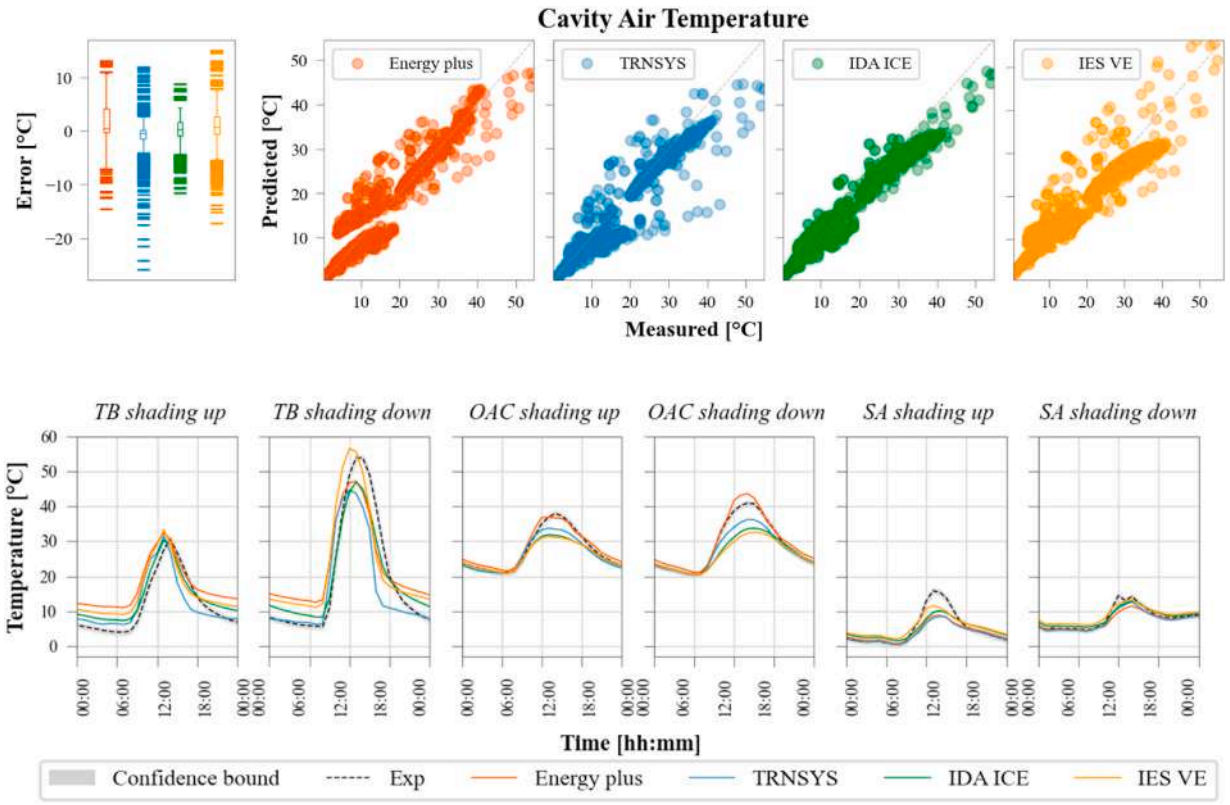

Fig. 9. Comparison between measured data and predicted outcomes of the cavity air temperature (up) – the six façade configurations are combined. Time profile of the cavity air temperature prediction and experimental data during the representative day of the datasets (down).

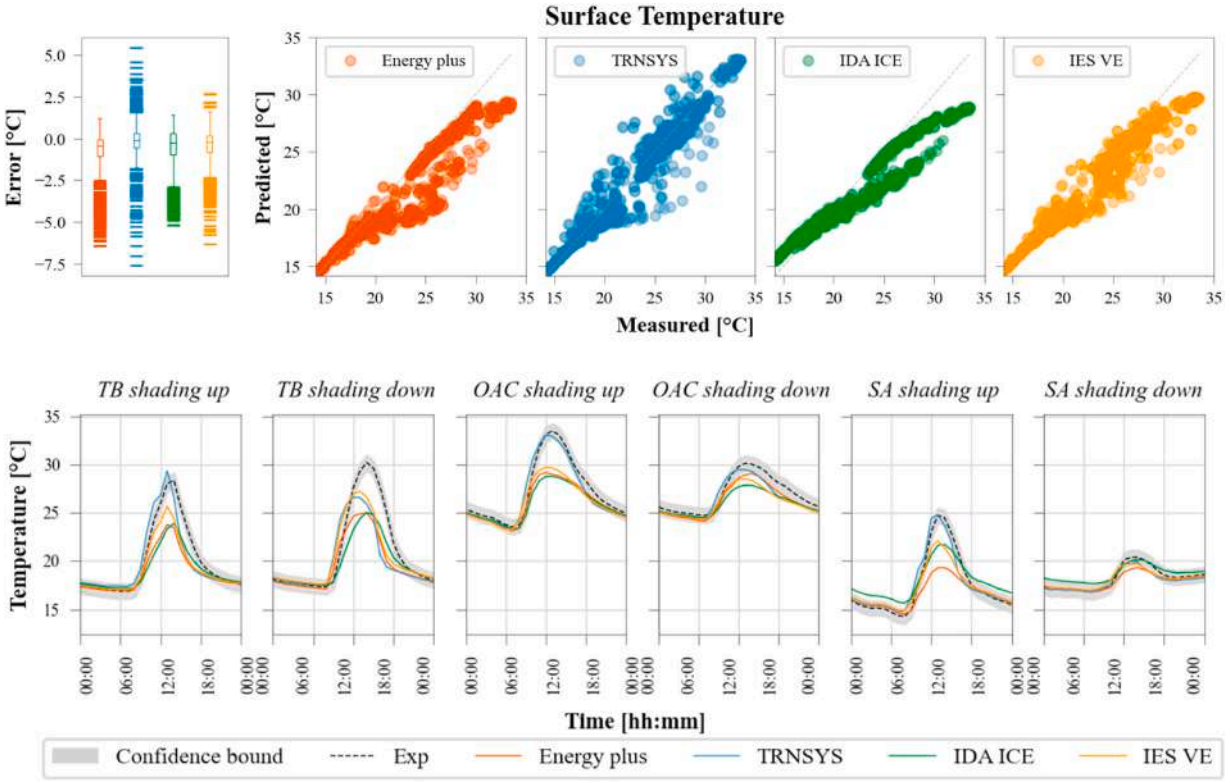

Fig. 10. Comparison between measured data and predicted surface temperature (up) outcomes – the six façade configurations are combined. Time profile of the surface temperature prediction and experimental data during the representative day of the datasets (down).

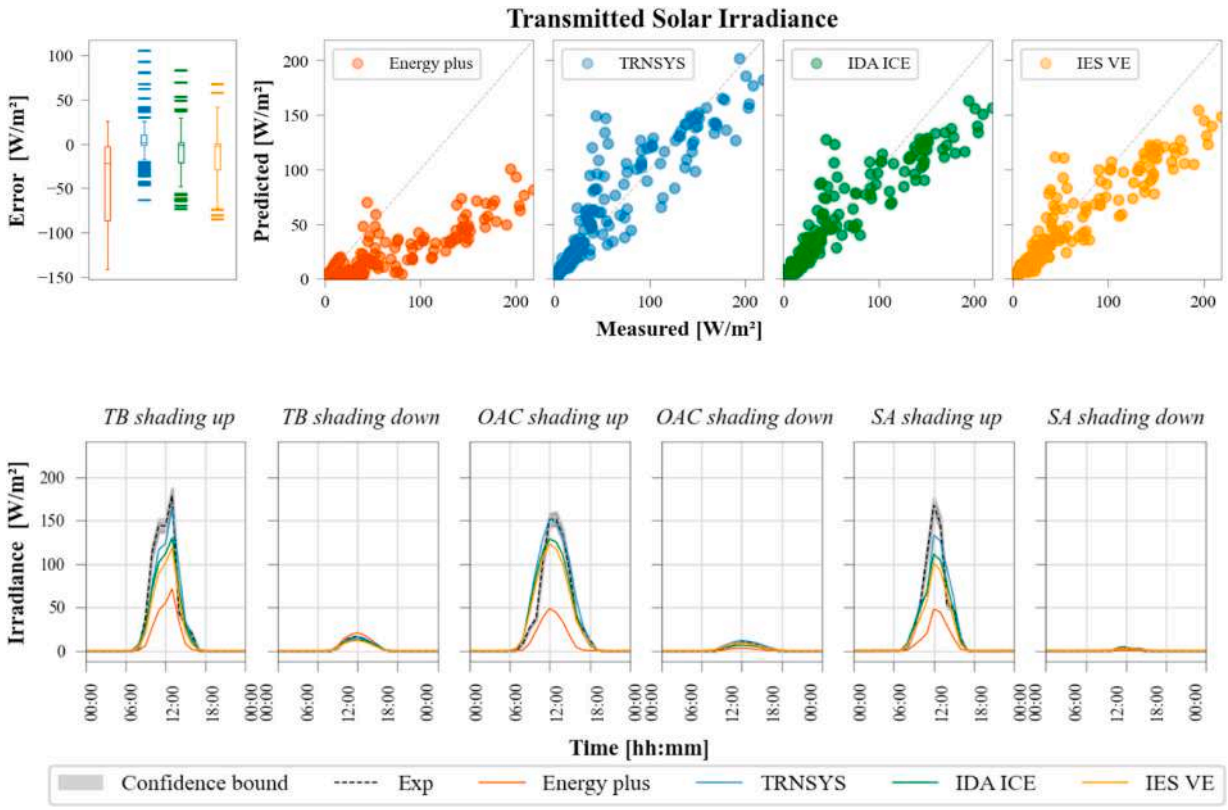

Fig. 11. Comparison between measured data and predicted outcomes of the transmitted solar irradiance (up) – the six façade configurations are combined. Time profile of the transmitted solar irradiance prediction and experimental data during the representative day of the datasets (down).

Table 3
MBE and RMSE values of the surface temperature calculated for the six DSF configurations.

	Surface Temperature [°C]											
	Thermal Buffer				Outdoor Air Curtain				Supply Air			
	MBE		RMSE		MBE		RMSE		MBE		RMSE	
Shading	down	up	down	Up	down	up	down	up	down	up	down	up
EnergyPlus	−1.3	−0.9	2.2	1.6	−0.7	−1.1	0.8	1.6	−0.3	−1.0	0.4	2.1
TRNSYS	−0.7	0.2	2.2	1.4	−0.5	−0.3	0.8	0.9	−0.2	0.1	0.4	0.7
IDA ICE	−1.0	−0.7	2.0	1.5	−0.9	−1.2	1.1	1.8	0.5	0.3	0.5	1.5
IES VE	−0.6	−0.4	1.9	1.2	−0.8	−1.0	1.0	1.6	−0.1	−0.3	0.3	1.1

Table 4
MBE and RMSE values of the transmitted solar irradiance calculated for the six DSF configurations.

	Transmitted solar irradiance [W/m^2]											
	Thermal Buffer				Outdoor Air Curtain				Supply Air			
	MBE		RMSE		MBE		RMSE		MBE		RMSE	
Shading	down	up	down	up	down	up	down	up	down	up	down	up
EnergyPlus	1.9	−42.4	2.5	56.5	−4.4	−76.9	5.1	81.3	−0.7	−64.4	1.7	82.5
TRNSYS	0.3	12.7	1.3	32.0	1.6	−6.1	1.7	16.7	1.3	−1.2	1.6	38.7
IDA ICE	−1.5	−3.2	2.1	28.9	−1.9	−12.6	2.5	20.3	0.9	−17.1	1.2	41.0
IES VE	−2.5	−11.7	2.9	31.3	−0.5	−19.4	1.2	26.0	0.6	−25.6	1.0	45.8

model, but this is not reflected in the statistical indicator (Table 3) as it shows a systematic underestimation of the temperature peaks during the daytime, whereas the quality of the prediction is drastically improved at night-time, as demonstrated by a much lower error during these periods.

The prediction of the solar irradiance transmitted through the double skin façade is shown in Fig. 11 and related statistical indicators in Table 4. The analysis is limited to the central hours of the day (11:00 and 15:00) to increase measurement accuracy, as explained in Section 3.1. TRNSYS offered the most accurate prediction of the transmitted solar irradiance in both solar shading configurations. A more accurate algorithm for solar distribution could be a contributing factor to this satisfactory result, as evidenced by the improvement in solar radiation modelling brought about by version 17 of TRNSYS, where a detailed beam and diffuse solar radiation model is available within the DSF cavity. On the other hand, IDA-ICE and IES-VE underestimated the high peaks during sunny days when the shading was retracted in a

comparable way. In contrast, EnergyPlus led to a great underprediction of the solar irradiance transmitted through the façade. In fact, although the most complex solar distribution model was adopted, among the options proposed by EnergyPlus, this direct and diffuse solar radiation distribution method does not allow description of the complex short-wave radiative heat transfer through the cavity for the zonal approach. Previous work has already assessed unsatisfactory performance [11], where it was highlighted that EnergyPlus offers the most accurate prediction of transmitted solar irradiance, but only when the in-built component approach is adopted (*Airflow window model*). Nevertheless, such a model can only be adopted to model mechanically ventilated DSFs.

In conclusion, it is not possible to identify a tool that outperforms the others for all the analysed quantities and DSF ventilation modes. The comparison with experimental data has revealed that cavity air temperature is the least accurate variable in all software on the basis of underestimation of the daytime peaks. Analysing the time profiles in Fig. 9, EnergyPlus is the most accurate software for cavity air temperatures in OAC mode, while IES-VE seems the most accurate for SA and TB mode (only when the shading is deployed). Regarding surface temperatures and transmitted solar radiation, TRNSYS appears to be the best-performing software, providing satisfactory results in line with experimental data regarding peak magnitude and dynamics.

Although IDA-ICE is the only software which provides the in-built module and considers the thermal inertia of the fenestration elements, this is not evident from the results due to the underestimation of peak temperatures during daytime in all the DSF configurations analysed.

Regarding SA mode, EnergyPlus completely fails to predict cavity air and surface temperature. This is due to the inability of the software to properly consider the airflow direction between the DSF cavity and the adjacent thermal zone (and not vice-versa). Although it was shown that CONTAM could enable a more accurate prediction, the simulation results were not entirely satisfactory. Moreover, the limitation of EnergyPlus in estimating the transmitted solar radiation in the zonal approach, due to the high impact of solar radiation over the other variables, is a potential cause of inconsistency between the measurements and the simulation outputs for the inner glazing surface temperature, and indirectly for the cavity air temperature.

Table 5 provides an overview of the findings of this investigation for the four BES tools analysed. The colour of the cell indicates how accurate the prediction was, while the sign indicates whether the tool underestimated or overestimated the experimental results. For performance detection, we have defined four error ranges: *good agreement* (green) if the temperature error is less than 1 °C (15W/m^2 for solar irradiance), *small error* (yellow) if the temperature error is less than 5 °C (25W/m^2 for solar irradiance), *moderate error* (orange) if the temperature error is less than 10 °C (50W/m^2 for solar irradiance), *large error* (red) otherwise. As for previous work [11], the error between the simulated and measured peaks was considered for judging the overall BES performance in Table 5.

5. Discussion

In this section, the challenges modellers may face when simulating a naturally ventilated DSF (cf. Section 2.2) are discussed and investigated using our modelling and building physics knowledge. Given that no BES tools performed significantly better than the others for all the DSF configurations, we chose the most appropriate DSF airpath configuration and BES tool to address each modelling challenge by means of a one-factor-at-the-time sensitivity analysis. The variable considered for this discussion is primarily the cavity air temperature, as it is the most challenging value to predict accurately and the one most affected by modelling assumptions for the elements that interact with the cavity.

In the zonal approach, there is not a standardised approach when discretising the number of stacked zones for a single-storey DSF cavity (a minimum of one up to a maximum of six zones are adopted in the literature). A sensitivity analysis was carried out on the OAC model in EnergyPlus using one zone, three zones and six zones. Fig. 12.a shows that using a single zone to model the entire cavity is not enough to produce satisfactory results. Conversely, subdividing the cavity into six zones is not rewarded by an improvement in performance compared to the model with three stacked zones in determining the cavity outlet temperature. However, this can be useful to study the stratification of the air along with the cavity.

The influence of the cavity distributed *pressure losses* was investigated using the IES-VE model in OAC mode. The frictional losses along the cavity surfaces were accounted for in the model by considering a concentrated pressure loss, reducing the opening area of virtual surfaces along the cavity. Thereby reducing the free area separating the three stacked zones (perpendicular to the airflow) from 100%, to 25% and 50% of the cavity section. However, these fictitious elements did not significantly impact the prediction of the cavity air temperature (Fig. 12b), which was reduced by a maximum of 1 °C in the case of a free area to the airflow of 25% of the original section.

Similarly, *wind pressure coefficients* did not affect the BES tools' prediction to a great extent. IES-VE was used again to model the supply air mode with the shading up, as this is the configuration where it is reasonable to expect the greatest influence of the wind pressure field on the naturally-driven airflow across the cavity. IES-VE is the tool that provides the modeller with the most detailed choice of pre-set wind pressure coefficients among those employed in the study (according to the exposure and the building geometry). The effect of the *wind pressure coefficient* was explored by varying the exposure type from exposed, to semi-exposed and sheltered. The results in Fig. 12.c show that its impact on the cavity air temperature is negligible. However, it must be highlighted that the wind speed values recorded during the experiment were up to 2 m/s, hence the negligible impact might reflect the small range of wind speed boundary conditions measured.

In order to verify the influence of *inlet and outlet opening characteristics* on the cavity air temperature, the model implemented in TRNSYS in OAC mode was employed, and the opening factor of the ventilation

Table 5
Performance overview of the tools in the three different ventilation modes. The performance of the two shading modes is combined. - - - Very high underestimation; - - High underestimation; - Underestimation;; = Good Agreement; + Overestimation; ++ High Overestimation; +++ Very High Overestimation; Colour code: Red: large error; Orange: moderate error; Yellow: small error; Green: accurate prediction. [ ]* refers to the performance of EnergyPlus using the AirflowNetwork.

Tool	***EnergyPlus***			***TRNSYS***			***IDA ICE***			***IES VE***		
Ventilation mode	**TB**	**OAC**	**SA**	**TB**	**OAC**	**SA**	**TB**	**OAC**	**SA**	**TB**	**OAC**	**SA**
Air gap temperature [°C]	=	=	- [---]*	-	-	-	-	--	-	-	--	-
Surface temperature [°C]	-	-	- [---]*	=	=	=	-	-	-	-	-	-
Solar irradiance [W/m^2]	---	---	---	=	=	=	-	-	-	-	-	--

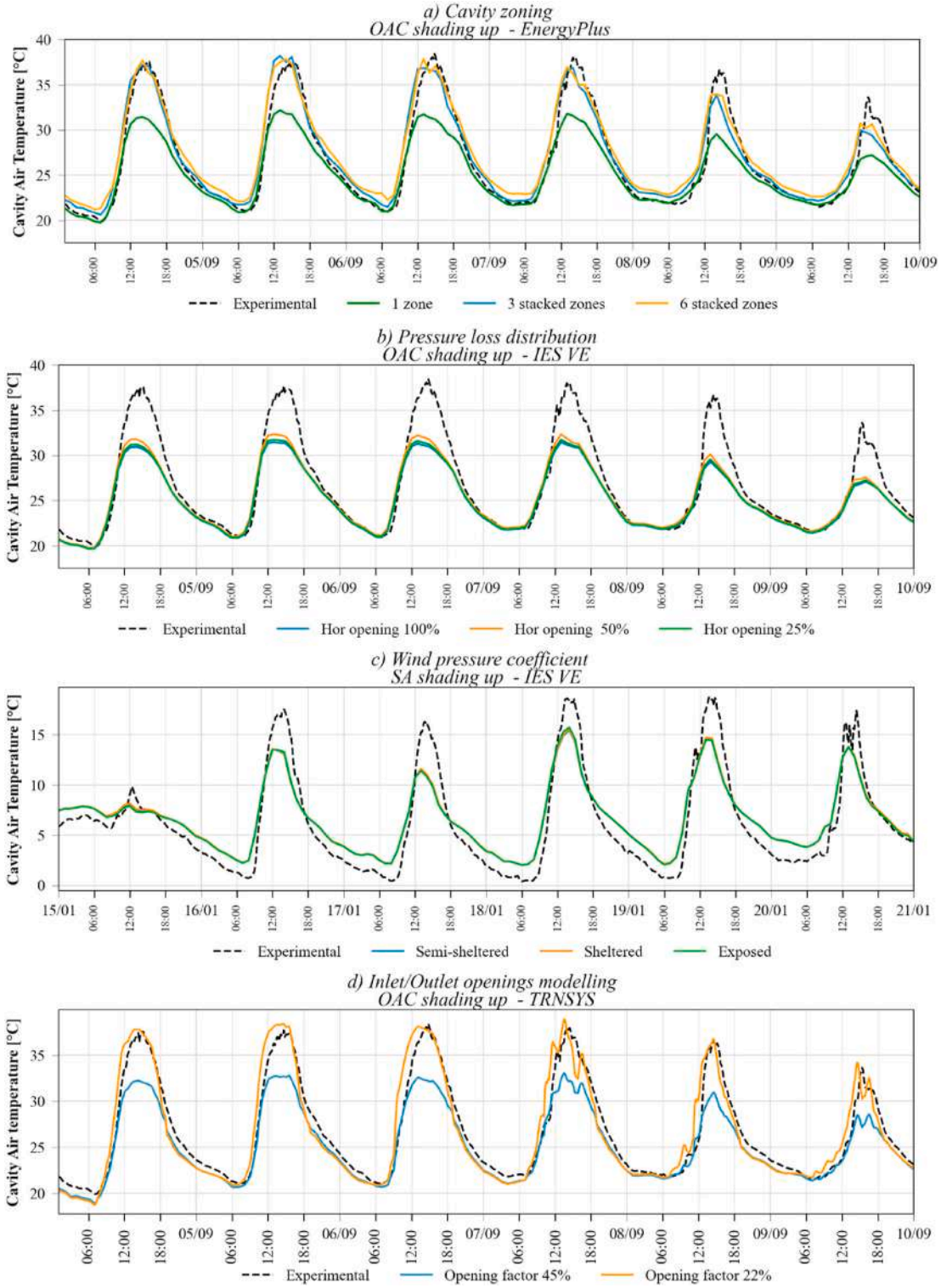

Fig. 12. Sensitivity analysis for zoning optimisation (a), pressure loss distribution (b), wind pressure coefficients (c), inlet and outlet modelling (d), air tightness of the inlet/outlet openings (e), convective heat transfer coefficient (f), capacitive node (g). Different tools and DSF modes have been used, as indicated in the graphs.

openings was varied by ±50% compared to the baseline value used for the investigation. The results shown in Fig. 12.d reveal that by decreasing the window opening, the error in predicting the cavity air temperature is reduced considerably. As explained in Section 4.5, TRNSYS, IES-VE and IDA-ICE tended to underestimate the peak of the cavity air temperature when the cavity was ventilated, especially in OAC mode. This is due to the complexity of estimating the free area of inlet and outlet apertures and related concentrated pressure losses, causing overestimation of the mass flow rate in the cavity within TRNSYS, IES-VE and IDA-ICE. Thus, it is evident that detailed studies on particular opening types should be carried out to model more accurately the flow through DSF cavities.

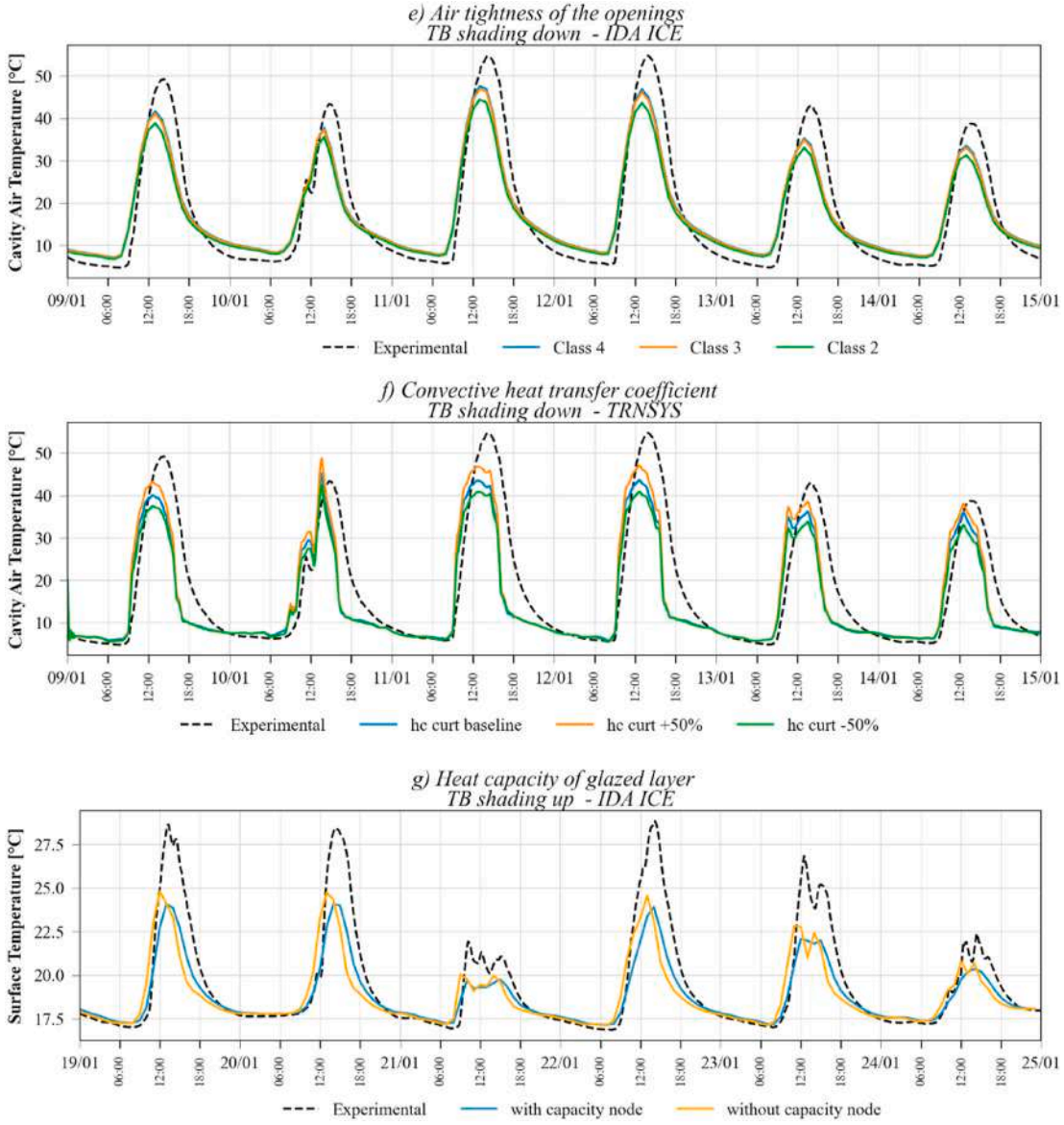

Fig. 12. (*continued*).

The impact of the *air tightness of the openings* was investigated using the model of IDA-ICE. The default leakage settings (0.5 ACH at 50 Pa) are applied only to the external surface corresponding to a window with a permeability of class 4 (3 $m^3/(h\ m^2)$) according to the EN12207:2016 [36]. In order to test the sensitivity of this parameter, the model was run adopting infiltration rates corresponding to class 3 (9 $m^3/(h\ m^2)$) and class 2 (27 $m^3/(h\ m^2)$). The results shown in Fig. 12.e reveal a minimal difference between classes 4 and 3, while higher infiltration rates corresponding to class 2 had a greater impact on the peak values of the cavity air temperatures for the analysed case (TB with shading device), with a reduction in the order of up to 2 °C.

One of the most challenging aspects of the heat transfer phenomena is the determination of the DSF cavity *convective heat transfer coefficients*. The cavity convective coefficient may significantly impact cavity air and surface temperatures. When a shading device is present, the convective heat exchange coefficient between the shading and the cavity air is probably even more relevant compared to that of the glazed surface, given the higher amount of solar irradiance absorbed (and released) by the shading device. For these reasons, a sensitivity analysis was carried out on the TB mode in TRNSYS by varying the convective heat transfer coefficient of the cavity-facing surface of the inner skin, and the convective heat transfer coefficient of the shading device separately. In the first analysis, the convective heat transfer coefficient was modified ±50%. The analysis shows that this variation of the convective coefficient has a minimal effect on the prediction of the DSF's thermophysical quantities, with a maximum improvement of 0.2 °C of the air cavity temperature. In the second analysis, the heat released by the shading device was modelled in simple terms in TRNSYS by varying the ratio between the radiative and the convective heat transferred from the shading. By varying the convective fraction by 50%, it was shown that the peak underestimation error is reduced by approximately 5 °C (Fig. 12f). Therefore, a change in the convective heat exchange is more relevant when applied to shading device than to the other surfaces facing the cavity.

Finally, neglecting the *glazing thermal inertia* by the window model of EnergyPlus, TRNSYS, and IES-VE caused a time-shift of the cavity dynamics (surface and air temperatures) compared to the experimental data as any heat absorbed by the glazed layer is instantaneously transferred to the air window cavity by convection and to the other surfaces by radiation. In the physical system, instead, the heat capacity of the glazed layers causes a delay between the solar radiation absorption and its re-emission via long-wave radiative heat transfer. This effect is

Table 6
Summary of findings from the sensitivity analysis.

Challenges	DSF mode	BES tool	Output Variable	Outcomes
Cavity zoning optimisation	OAC shading up	EnergyPlus	Cavity air temperature	Three stacked zones to divide the cavity may be sufficient
Pressure loss distribution in the cavity	OAC shading up	IES VE	Cavity air temperature	Minimal effect on the prediction
Wind pressure coefficient	SA shading up	IES VE	Cavity air temperature	Minimal effect on the prediction
Inlet/Outlet modelling	OAC shading up	TRNSYS	Cavity air temperature	Inlet/outlet opening factor reduced by half significantly improved results
Opening air tightness	TB shading down	IDA ICE	Cavity air temperature	Minimal effect on the prediction
Convective heat transfer coefficients	TB shading down	TRNSYS	Cavity air temperature	Increasing the convective coefficient of the shading device by 50% improved the estimation of peaks by 5 °C
Heat capacity of glazed layer	TB shading up	IDA ICE	Glazing Surface temperature	The absence of the capacitive node anticipates temperature peaks by 1 h

amplified in DSFs, where there might be a higher thermal mass due to the number and thickness of glass layers. This is particularly evident in Thermal Buffer mode since, apart from the infiltration, there is no mass exchange between the cavity and the boundary zones (indoor and outdoor). IDA-ICE allows the modeller to input values for the heat capacity of the glazed layers. In Fig. 12.g the hourly profiles of the simulated inner surface temperature with and without the glass's specific heat capacity are presented. The temperature profile in the case without the thermal mass of the glazing resembles the temperature outcomes of the other BES tools. In this case, indeed, the temperature peak was predicted approximately 1 h ahead of the measurement data. This limitation could be overcome by increasing the thermal capacity of the (cavity) air node, a feature controlled in both TRNSYS and EnergyPlus. However, such technical expedients are more of an art in nature than based on robust practices, which can work in case of calibration (with available experimental data to compare with), but it is difficult to employ them in a simulation task for system design. A summary of the results of the sensitivity analysis is reported in Table 6.

6. Conclusion

DSF design, due to its more complex behaviour compared to conventional building envelopes, cannot be based on simple performance parameters. It requires more detailed building performance simulation. The accuracy of BES tools in predicting the thermal behaviour of naturally ventilated double-skin façades is crucial in proving their performance and could boost their adoption in real buildings. Furthermore, BES could be used as virtual test beds to design and compare control strategies for DSFs, which are of utmost importance for increasing the whole building operational performance.

The findings of this comprehensive investigation indicate that no single BES tool outperforms the others for different DSF configurations. The cavity air temperature was the most difficult variable to predict: IES-VE provided good predictions in thermal buffer mode and EnergyPlus in outdoor air curtain mode, while the performance of all tools was quite similar for supply air mode– with the exception of EnergyPlus. The use of CONTAM in a co-simulation scheme was necessary to reduce the gap in the performance prediction. In most of the tools, the absence of heat capacity of the glazing system is reflected in a considerate lagging of the prediction of the peak compared to the experimental data. This effect was more pronounced in thermal buffer mode since the thermal behaviour is governed by the heat transfer between the façade system and the cavity air (the mass exchange is minimal in this configuration). The effect is particularly noticeable when the roller shade is deployed. For the other ventilation modes, TRNSYS, EnergyPlus and IDA-ICE tended to underpredict the peak cavity temperature when the shading was deployed, whilst the performance of IES-VE was unaltered. TRNSYS, instead, performed better in predicting the surface temperature and the transmitted solar irradiance, providing satisfactory results in line with experimental data.

With the exception of IDA-ICE, in most BES tools, the zonal approach is the only alternative to model naturally a ventilated DSF. This requires expert knowledge of physical phenomena to understand the simulated results' reliability, going beyond the default parameters, as demonstrated by the modelling, experimental validation and sensitivity analysis carried out. Moreover, building energy simulations often require input data that is not easily accessible from technical drawings, so modellers must devise abstractions and workarounds based on their experience.

Therefore, sensitivity analyses were conducted to discuss the influence of unknowns and challenges modellers may face when simulating a naturally ventilated DSF. The investigation proved that the aspects impacting most the thermal behaviour of the DSF are the ones directly affecting the mass flow in the cavity for ventilated configurations (outdoor air curtain and supply air) and the ability of the model to represent the thermal inertia of the glazing system for thermal buffer mode. The biggest challenge is probably the accurate estimation of inlet/outlet opening areas and related ventilation opening models implemented in the BES tools. In addition, when the shading was present, current correlations employed to calculate the convective heat exchange between the shading and the cavity air led to the underestimation of air temperature in the cavity. Moreover, the ability to account for the heat capacity of the glass layers results in a better estimation of the temperature dynamics within the DSF models. These aspects can represent directions for future work and model development to improve the performance prediction of DSF in BES tools. Finally, providing the modellers with an increased number of BES output variables, especially when it comes to the zonal approach, could contribute to improving the confidence in the results by offering more opportunities for validation and model debugging (i.e. variables such as cavity air velocity and transmitted solar radiation between adjacent internal zones). In light of the above, both the models and the experimental data generated for the present study are publicly and freely available on an open-access repository:

- the models developed with the different simulation environments for this study can be found at, and referenced using, the following https://doi.org/10.5281/zenodo.7437314 [37];
- the experimental data generated for this study, for the validation of the models, can be found at, and referenced using, the following https://doi.org/10.5281/zenodo.7436983 [38].

CRediT authorship contribution statement

Giovanni Gennaro: Writing – original draft, Visualization, Validation, Methodology, Investigation, Formal analysis, Data curation, Conceptualization, Software, Writing – review & editing. **Elena Catto Lucchino:** Writing – original draft, Validation, Formal analysis, Data curation, Conceptualization, Investigation, Methodology, Software, Writing – review & editing. **Francesco Goia:** Writing – review & editing, Supervision, Resources, Project administration, Methodology, Funding

acquisition, Conceptualization, Visualization. **Fabio Favoino:** Writing – review & editing, Visualization, Supervision, Resources, Methodology, Funding acquisition, Conceptualization.

Declaration of competing interest

The authors declare that they have no known competing financial interests or personal relationships that could have appeared to influence the work reported in this paper.

Data availability

We make available on ZENODO, an open-access repository, the models developed with the different simulation environments and the experimental data generated.

Acknowledgements

The authors would like to acknowledge the Research Council of Norway for sponsoring the research project "REsponsive, INtegrated, VENTilated - REINVENT – windows" (research grant no. 262198) and Hydro Extruded Solutions for the realisation and installation of the DSF prototype.

The authors thank the Department of Innovation, Research and University of the Autonomous Province of Bozen/Bolzano for covering the Open Access publication costs.

Appendix A

A description of the physical-mathematical models for energy and mass balance, and for heat transfer processes relevant for the simulation of DSF systems have been presented in a previous study – [11], see Appendix B – for the four BES tools employed in the study. For the sake of brevity, the focus in this Appendix will be placed on the distinctive aspects that play a role in the modelling of natural ventilation and on how the models have been set up to represent the particular test case adopted in this study. The reader might therefore find useful to first go through the description of the physical-mathematical models in Ref. [11] to have a complete overview of how DSFs can be modelled in the different BES tools.

A.1 - EnergyPlus

The model geometry of the case study was first defined in SketchUp through the Euclide plug-in. SketchUp allows the user to define the three stacked zones for the façade and one zone for the indoor environment and automatically matches surfaces between zones. The cavity zone was modelled with exterior and interior double glazing, whilst the inlet and outlet were provided with the ventilation opening modelled as opaque doors. The surface between each stacked zone was modelled as a fictitious window made of infrared transparent material. The other surface of the zones, which corresponds to the frame of the façade, was modelled as massive construction with defined stratigraphy.

The airflow between the stacked zone and the adjacent internal zone was modelled and managed through the Airflow Network, in which each zone corresponds to a single air node linked by airflow components. The fictitious surface zone divider was modelled as an always-open horizontal opening, while pivoted windows were used as ventilation openings to link the façade nodes with the outdoor and indoor nodes. In the pivoted windows, the opening angle is linearly proportional to the window opening factor (an opening factor of 1 equals an opening angle of 90°), and by varying this factor it was possible to open and close the ventilation openings, which were managed by the EMS tool through input schedules, in order to indicate the DSF airpath configuration to simulate.

"*Full interior and exterior with reflections*" was used as the solar distribution algorithm to calculate the interior solar radiation distribution. As a result, transmitted beam solar radiation is divided into each surface in the zone by projecting the sun's rays through the exterior windows, taking into account the effect of the window shading devices. The shading was modelled as a window shade material and assigned to the exterior window as an interior shading device 12.25 cm from the glass surface (middle of the air cavity). The convection coefficient for the cavity surfaces was calculated according to the ISO 15099 [30], chosen automatically by the "*adaptive algorithm*".

Co-simulation between EnergyPlus and CONTAM

The CONTAM user interface, ContamW, was used to create the CONTAM project file containing a scaled representation of the test cell. The cavity and the indoor room were divided into three stacked zones belonging to three different levels. The fictitious zone dividers were modelled as "*Shaft*" elements always opened, while the ventilation openings were modelled as "*Two-way Flow Opening*" elements. Each of these elements requires the geometry of the openings (in terms of cross-sectional area and perimeter for the Shaft elements and height and width for the ventilation openings), the flow exponent (set to 0.5 – default value) and the distance between the floor's level. In addition, for the ventilation openings the discharge coefficient is also required, which was set to 0.65. Finally, the fictitious duct connecting the volume of the test cell to the outdoor was modelled as an "*Orifice area*" with a 0.1 m^2 cross-sectional area.

Starting from the CONTAM project file, the CONTAM3Dexporter was used to generate an IDF file containing building geometry with the construction and the zone infiltration objects. At each simulation time step EnergyPlus gets interzone and infiltration airflows from CONTAM, while CONTAM successively receives indoor air temperature from EnergyPlus and performs airflow simulation. The co-simulation is performed using the Functional Mock-up Unit (FMU), in which EnergyPlus implements a co-simulation master algorithm and CONTAM is a slave process.

A.2 - TRNSYS

The model geometry of the case study was defined in the 3D Building plug-in for SketchUp, which allows the user to define the three stacked zones for the façade and one zone for the indoor environment and to match surfaces between zones automatically. The openings between each stacked zone were modelled as virtual surfaces in order to merge the three air nodes into a single thermal zone. Indeed, TRNSYS distinguishes between zones and air nodes: TRNFLOW interacts with the air nodes, whilst the radiation balance is solved for thermal zones. Thus, the DSF was modelled as one thermal zone containing several stacked air nodes linked with large virtual openings. The DSF air nodes network was linked with the whole building air nodes network so that the DSF became an integrated part of the building.

TRNSYS uses TRNFLOW [19] to integrate the multizone airflow model COMIS into the thermal building module (Type 56). All the ventilation openings were modelled as large pivoted windows whose dimensions replicate the size of the opening size of the case study (1.4 m width and 0.3

height) and the fictitious openings between cavity air nodes were modelled as always-opened large windows, corresponding to the cavity dimensions. In order to make the DSF model flexible, the opening factor of the window (0 for closed and 0.45 for open) was given to TRNFlow as input through Type 9.

The "*detailed radiation model*" was used for shortwave direct and diffuse radiation distribution and long-wave radiation exchange within a zone, as recommended in Ref. [19] for simulating a double-skin façade and atrium. Using the 3D geometry, the model allows for detailed solar distribution, including reflections in the zone cavity. In particular, for the distribution of the beam radiation, matrices based on the 3D dimensional data of the building are used to distribute the primary solar direct radiation entering the zone; for diffuse and long-wave radiation, the radiation model applies the so-called Gebhart factor [19] to generate the view factor matrix.

The shading was assigned to the exterior window as an interior shading device. Therefore, it is not possible to define the position of the shading, and the model allows only to define the fraction of the solar radiation absorbed by the internal device that is transferred by convection to the cavity air between the inner window pane and the internal shading device (this value was set to 0.5 as default).

The internal convective heat transfer coefficient was calculated using the vertical window's internal algorithm.

A.3 - IES VE

The model was created employing IES VE 2021. The modelling of the double-skin façade was obtained using different stacked thermal zones. The '*Apache*' module was used to assign the building's thermal properties and solve the thermal network. The '*MacroFlo'* module was used to define the openings and model the airflow network. The '*ApacheSim'* simulation engine determines the building's thermal conditions by balancing sensible and latent heat flows entering and leaving each air mass and building surface. ApacheSim uses a stirred tank model of the air in a room. Since *ApacheHVAC* and *MacroFlo* are included, the calculations also include the mechanical and natural ventilation airflow rates calculated by these tools and the inter-dependence between these variables and those calculated within ApacheSim.

The DSF was modelled as three stacked zones delimited by two horizontal windows modelled as holes (always open and transparent to solar radiation). The inlet and outlet openings were modelled as large openings using the window category '*Top- Hung'*. The default coefficients were adopted to model the closed opening (Crack Flow 0.015 l/(s*m*Paˆ0.6)).

The shading device was assigned to the internal side of the external glazing system, and it is not possible to define the distance from the glass. It was modelled as an internal curtain and the values of shading coefficient (SC) and shortwave radiant fraction coefficient (SWRF) were calculated starting from the absorption and transmission values of the shading device [17]:

$$SC = \tau + 0.87\alpha;\ SWRF = \frac{\tau}{SC}$$

The inner surface's convection coefficient of the DSF was calculated using Alamdari and Hammond's correlation [30].

A.4 - IDA ICE

The model was developed using IDA ICE 4.8, and the in-built component '*Double-Glass Façade'* was used to model the ventilated cavity. The façade was modelled as a '*Ventilated wall'*, which means that the entire façade is modelled as ventilated. The glazing, both internal and external, was modelled using the detail window component that models the window panes and shading layer according to the ISO 15099 [14].

Due to the geometry of the experimental set-up, some adjustments concerning the frame ratio were necessary; the interior window was modelled as a window with dimensions corresponding to the glazed area and 1% frame. The wall on which this window is installed was modelled with a U-value corresponding to the one of the window frames. The exterior window was instead modelled as the real one (full height and 60% of the frame). This workaround was necessary to overcome the tool limitations when distributing the solar radiation from the exterior window to the inner glazing. The calculation methods applied in the '*detailed window model'* assume a geometrical distribution between the glazing and the frame, not as a function of the incident angle. This leads to a sub-optimal distribution of the solar radiation on the inner glazing, thereby significantly underestimating the solar radiation transmitted by the whole component (only 40% of the radiation would be hitting the inner glass). Since the two glazing panes are very close, it can be assumed that a higher percentage of radiation that penetrates the first skin also crosses the second. This distribution cannot be modified if the inner facade is modelled as a whole façade window since the distribution between glazing and frame is done within the "*detail window component*", while the amount of solar distributed to the inner walls of the cavity can be modified instead. Therefore, by assigning the thermal properties of the frame to the wall and modelling the window as almost 100% glazed, it was possible to redistribute the solar radiation with a more realistic ratio (70% to the glazing and 30% to the frame).

The shading device was modelled as part of the exterior glazing and placed 12.5 cm from the inner pane. For both glazing systems, the capacity of each glass pane was set to 750 J/kg K.

The indoor and outdoor openings (according to which configuration was modelled) were modelled as leaks. Therefore, the default effective leakage area (ELA) method was adopted. The ELA values used were calculated using the method described in the TRNSYS manual for hinged windows [19]. To model the infiltration, the tool default assumption was adopted when the windows were closed (0.5 ACH at 50 Pa). This means that, if applied to a single exposed façade, the total ELA was $2x10^{-4}$ m^2, if distributed to the two openings, it corresponds to 10^{-4} m^2 each.

References

[1] A. GhaffarianHoseini, A. GhaffarianHoseini, U. Berardi, J. Tookey, D.H.W. Li, S. Kariminia, Exploring the advantages and challenges of double-skin facades (DSFs), Renew. Sustain. Energy Rev. 60 (2016) 1052–1065, https://doi.org/10.1016/j.rser.2016.01.130.

[2] F. Favoino, M. Baracani, L. Giovannini, G. Gennaro, F. Goia (2022). 6 - Embedding Intelligence to Control Adaptive Building Envelopes, Editor(s): Eugenia Gasparri, Arianna Brambilla, Gabriele Lobaccaro, Francesco Goia, Annalisa Andaloro, Alberto Sangiorgio, In Woodhead Publishing Series in Civil and Structural Engineering, Rethinking Building Skins, Woodhead Publishing, 2022, Pages 155-179, ISBN 9780128224779, https://doi.org/10.1016/B978-0-12-822477-9.00007-3.

[3] R.C.G.M. Loonen, F. Favoino, J.L.M. Hensen, M. Overend, Review of current status, requirements and opportunities for building performance simulation of adaptive facades, J. Build. Perform. Simul. 10 (2) (2017) 205–223, https://doi.org/10.1080/19401493.2016.1152303.

[4] W. Choi, J. Joe, Y. Kwak, J.H. Huh, Operation and control strategies for multi-storey double skin facades during the heating season, Energy Build. 49 (2012) 454–465, https://doi.org/10.1016/j.enbuild.2012.02.047.

[5] I. Khalifa, L. Gharbi-Ernez, E. Znouda, C. Bouden, Assessment of the inner skin composition impact on the double-skin façade energy performance in the

mediterranean climate, Energy Proc. 111 (2017) 195–204, https://doi.org/10.1016/j.egypro.2017.03.021. September 2016.
[6] N.M. Mateus, A. Pinto, G.C. Da Graça, Validation of EnergyPlus thermal simulation of a double skin naturally and mechanically ventilated test cell, Energy Build. 75 (2014) 511–522, https://doi.org/10.1016/j.enbuild.2014.02.043.
[7] A.S. Ancrossed D Signelković, I. Mujan, S. Dakić, Experimental Validation of a EnergyPlus Model: Application of a Multi-Storey Naturally Ventilated Double Skin Façade, vol. 118, Energy Build, 2016, pp. 27–36, https://doi.org/10.1016/j.enbuild.2016.02.045.
[8] M. Shahrestani, et al., Experimental and numerical studies to assess the energy performance of naturally ventilated PV façade systems, Sol. Energy 147 (2017) 37–51, https://doi.org/10.1016/j.solener.2017.02.034.
[9] D. Kim, S.J. Cox, H. Cho, J. Yoon, Comparative investigation on building energy performance of double skin façade (DSF) with interior or exterior slat blinds, J. Build. Eng. 20 (2018) 411–423, https://doi.org/10.1016/j.jobe.2018.08.012. January.
[10] D.W. Kim, C.S. Park, Difficulties and limitations in performance simulation of a double skin façade with EnergyPlus, Energy Build. 43 (12) (2011) 3635–3645, https://doi.org/10.1016/j.enbuild.2011.09.038.
[11] E. Catto Lucchino, et al., Modelling double skin façades (DSFs) in whole-building energy simulation tools: validation and inter-software comparison of a mechanically ventilated single-story DSF, Build. Environ. 199 (2021), https://doi.org/10.1016/j.buildenv.2021.107906. November 2020.
[12] E. Catto Lucchino, F. Goia, G. Lobaccaro, G. Chaudhary, Modelling of double skin facades in whole-building energy simulation tools: a review of current practices and possibilities for future developments, Build. Simulat. 12 (1) (2019) 3–27, https://doi.org/10.1007/s12273-019-0523-7, 10.1007/s12273-019-0511-y)," Build. Simul., pp. 3–27, 2019.
[13] J. Hensen, M. Bartak, F. Drkal, Modeling and simulation of a double-skin façade system, Build. Eng. 108 (2002). January.
[14] A.B. Equa Simulation, IDA ICE 4, 8 User Manual," No, 2018. January,.
[15] U. S. DOE, Engineering Reference, 2014.
[16] M. Hiller, J. Merk, P. Schöttl, TRNSYS 18 - Type 56: Complex Fenestration Systems Tutorial, 2017, pp. 1–22. January.
[17] V.E. Ies, ApacheSim User Guide," *IES VE User Guide*, 2014.
[18] G.N. Walton, Airnet - a computer program for building airflow network modelling, Nistir 89-4072 77 (1989) no. April.
[19] Solar Energy Laboratory, Trnsys 18, Vol. 5 Multizone Build. Model. with Type 56 TRNBuild 3 (2018) 7–36.
[20] P. Warren, Multizone air flow modelling (COMIS, Int. Energy Agency 48 (2000).
[21] E. Taveres-Cachat, F. Favoino, R. Loonen, F. Goia, Ten questions concerning co-simulation for performance prediction of advanced building envelopes, Build. Environ. 191 (2021), 107570, https://doi.org/10.1016/j.buildenv.2020.107570. January.
[22] W.S. Dols, B.J. Polidoro, CONTAM User Guide and Program Documentation, 2020, p. 330, https://doi.org/10.6028/NIST.TN.1887r1. https://nvlpubs.nist.gov/nistpubs/TechnicalNotes/NIST.TN.1887r1.pdf [Online]. Available:, Version 3.4.
[23] W.S. Dols, S.J. Emmerich, B.J. Polidoro, Coupling the multizone airflow and contaminant transport software CONTAM with EnergyPlus using co-simulation, Build. Simulat. 9 (4) (2016) 469–479, https://doi.org/10.1007/s12273-016-0279-2.
[24] M. Justo Alonso, W.S. Dols, H.M. Mathisen, Using Co-simulation between EnergyPlus and CONTAM to evaluate recirculation-based, demand-controlled ventilation strategies in an office building, Build. Environ. 211 (2022), 108737, https://doi.org/10.1016/j.buildenv.2021.108737.
[25] I. Khalifa, L.G. Ernez, E. Znouda, C. Bouden, Coupling TRNSYS 17 and CONTAM: simulation of a naturally ventilated double-skin façade, Adv. Build. Energy Res. 9 (2) (2015) 293–304, https://doi.org/10.1080/17512549.2015.1050694.
[26] N. Yoon, D. Min, Y. Heo, Dynamic compartmentalization of double-skin façade for an office building with single-sided ventilation, Build. Environ. 208 (September 2021) (2022), 108624, https://doi.org/10.1016/j.buildenv.2021.108624.
[27] ASHRAE, 2001 Fundamental Handbook 30 (2001).
[28] M.W. Liddament, Air Infiltration Calculation Techniques - an Application Guide, Air Infiltration and Ventilation Centre, 1986.
[29] ASHRAE, ASHRAE fundamental handbook, Atlanta 30 (2001).
[30] ISO 15099, "International Standard ISO 15099:2003., Thermal Performance of Windows, Doors and Shading Devices — Detailed Calculations, 2003.
[31] F. Alamdari, G.P. Hammond, Improved data correlation for buoyancy-driven convection in rooms, Build. Serv. Eng. Technol. 4 (3) (1983) 106–112.
[32] A. Jankovic, G. Gennaro, G. Chaudhary, F. Goia, F. Favoino, Tracer gas techniques for airflow characterization in double skin facades, Build. Environ. 212 (2022), 108803, https://doi.org/10.1016/j.buildenv.2022.108803. January.
[33] F. Favoino, F. Goia, M. Perino, V. Serra, Experimental analysis of the energy performance of an ACTive, RESponsive and Solar (ACTRESS) façade module, Sol. Energy 133 (2016) 226–248, https://doi.org/10.1016/j.solener.2016.03.044, 2016.
[34] F. Goia, V. Serra, Analysis of a non-calorimetric method for assessment of in-situ thermal transmittance and solar factor of glazed systems, Sol. Energy 166 (2018) 458–471, https://doi.org/10.1016/j.solener.2018.03.058. November 2017.
[35] ASHRAE, Guideline 14-2014, Measurement of Energy and Demand Savings, Atlanta, 2014.
[36] EN 12207 Windows and Door Air Permeability Classification, 2016.
[37] G. Gennaro, E. Catto Lucchino, F. Goia, F. Favoino, Models for Validation of a Naturally Ventilated Single-Story Double Skin Facade in Whole-Building Energy Simulation Tools, 2022, https://doi.org/10.5281/zenodo.7437314.
[38] G. Gennaro, E. Catto Lucchino, F. Goia, F. Favoino, Experimental Data for Validation of a Naturally Ventilated Single-Story Double Skin Facade in Whole-Building Energy Simulation Tools, 2022, https://doi.org/10.5281/zenodo.7436983.
[39] J.M. Bright, N.A. Engerer, Engerer2: global re-parameterisation, update, and validation of an irradiance separation model at different temporal resolutions, J. Renew. Sustain. Energy 11 (3) (2019), https://doi.org/10.1063/1.5097014.
[40] J.-N. Hersbach, H, B. Bell, P. Berrisford, G. Biavati, A. Horányi, J. Muñoz Sabater, J. Nicolas, C. Peubey, R. Radu, I. Rozum, D. Schepers, A. Simmons, C. Soci, D. Dee, Thépaut, ERA5 hourly data on single levels from 1979 to present. Copernicus Climate Change Service (C3S) Climate Data Store (CDS) (2018), https://doi.org/10.24381/cds.adbb2d47. Accessed on < 26-APR-2021 >).